TRENDS IN INDIAN SUMMER MONSOON DISTRIBUTION OVER THE WESTERN GHATS

By

ABHIJIT ASOKAN

2011-20-109

THESIS

Submitted in partial fulfilment of the requirements for the degree

B.Sc.-M.Sc. (Integrated) Climate Change Adaptation

Faculty of Agriculture

Kerala Agricultural University

ACADEMY OF CLIMATE CHANGE EDUCATION AND RESEARCH

VELLANIKKARA, THRISSUR - 680 656

KERALA, INDIA

2016

DECLARATION

I hereby declare that the thesis entitled **"Trends in Indian Summer Monsoon Distribution over the Western Ghats"** is a bonafide record of research work done by me during the course of research and the thesis has not been previously formed the basis for the award to me any degree, diploma, fellowship or other similar title, of any other University or Society.

Vellanikkara
Date: 10/11/16

ABHIJIT ASOKAN
(2011-20-109)

CERTIFICATE

Certified that this thesis entitled **"Trends in Indian Summer Monsoon Distribution over the Western Ghats"** is a record of research work done independently by Mr. Abhijit Asokan under my guidance and supervision and that it has not previously formed the basis for the award of any degree, diploma, fellowship or associateship to him.

Vellanikkara

Date: 23/11/16

Dr. E. K. Kurien
(Chairman, Advisory Committee)
Special officer,
Academy of Climate Change Education and Research,
Kerala Agricultural University,
Thrissur

CERTIFICATE

We, the undersigned members of the advisory committee of Mr. Abhijit Asokan, a candidate for the degree of B.Sc.-M.Sc. (Integrated) Climate Change Adaptation, agree that the thesis entitled **"Trends in Indian Summer Monsoon Distribution over the Western Ghats"** may be submitted by Mr. Abhijit Asokan (2011-20-109), in partial fulfilment of the requirement for the degree.

Dr. E. K. Kurien
Professor and Special Officer,
ACCER, Kerala Agricultural University, Thrissur

20/MAR/2017
Dr. Sachin S. Gunthe
Scientist,
Environment and Water Resource Engineering Division,
Civil Engineering Department,
Indian Institute of Technology,
Chennai

Dr. K. M. Sunil
Assistant Professor (Agricultural Meteorology),
Krishi Vigyan Kendra,
Pattambi

Dr. Mary Regina F.
Professor (Soil and Water Engineering),
Krishi Vigyan Kendra, Thrissur

16/12/17
External Examiner (Dr. Jobi V. Paul)

ACKNOWLEDGEMENTS

At the outset, I would like to express my gratitude to Dr. Sachin S. Gunthe., Scientist, EWRE, IIT Madras for his exceptional guidance and relentless inspiration throughout the period of my M.Sc. thesis. It was a great honor and privilege working under his guidance.

I am thankful to Kerala Agricultural University, Academy of Climate Change Education and Research, and Environment and Water Resources Engineering Division at the Civil Engineering Department of IIT, Madras for giving me an opportunity to work in this area of research.

I am grateful to Dr. E. K. Kurien, Special officer, Academy of Climate Change Education and Research, KAU and my major advisor who served as my thesis supervisor for his timely guidance and ideas. I cannot thank him enough for his encouragement in successful completion of this project.

I express my thanks to Dr. K. M. Sunil, Assistant Professor, (Agricultural Meteorology) and member of my advisory committee for his scrupulous guidance, advices, valuable and timely suggestions given during my work.

I express my thanks to Dr. Mary Regina F. Professor (Soil and Water Engineering) Krishi Vigyan Kendra, Thrissur and member of my advisory committee for her advices and timely suggestions.

I express my gratitude to Dr. Shaji James P., Professor, KCAET, Tavanur and Dr. K. P. Sudheer, EWRE, IIT, Madras for giving me an opportunity to work in this area. I am also thankful to Ms. Saimy Davis, Research scholar, IIT, and Dr. T. Thomas, Scientist, National Institute of Hydrology for their constant support and help.

I am short of words to extent my gratitude to my small family, SPARTANS-2011, for their support given to me during the whole college days.

I would like to thank my sister and brother without whom this wouldn't have been possible.

I would like to dedicate this thesis to my family who have always supported me in my endeavors and have had an unfaltering confidence in my abilities and skills.

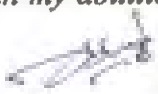

Abhijit Asokan

TABLE OF CONTENTS

LIST OF TABLES

LIST OF FIGURES

SYMBOLS AND ABBREVIATIONS

AR	Assessment Report
AZB	Amman Zarqa Basin
CNE	Central North-East India
ENSO	El-Nino Southern Oscillation
EVT	Extreme Value Theory
GCM	Global Circulation Model
GEV	Generalized Extreme Value
GPD	Generalized Pareto Distibution
GHG	Green House Gas
IGP	Indo Gangetic Plains
IMD	India Meteorological Department
IPCC	Inter-Governmental Panel on Climate Change
ISMR	Indian Summer Monsoon Rainfall
ITCZ	Inter Tropical Convergence Zone
KS	Kolmogorov-Smirnov
ODMR	One Day Maximum Rainfall
Q-Q	Quantile-Quantile
RF	Radiative Forcing
SST	Sea Surface Temperature
UNESCO	United Nations Educational, Scientific and Cultural Organization
UNFCCC	United Nations Framework Convention on Climate Change
WCA	West Coast of India and adjoining eastern Arabian Sea
WG	Western Ghats

CHAPTER 1

INTRODUCTION

The hill chain of the Western Ghats, a treasure trove of biodiversity and the water tower of Peninsular India, runs parallel to the west coast of India from the river Tapi in the north to Kanyakumari in the south. Western Ghats along with North-East region of India are the two locations which receive highest annual rainfall in India. Both of these regions have unique characteristic of mountainous terrain. This hilly terrain acts as a barrier to south west winds coming from Arabian Sea leading to intensified downpour at the windward side of the mountains. The Ghats with its strategic position plays a great role in channelling the summer monsoonal rain into the mainland. The area encompassed by the Ghats and the coast through its topography, vegetation and orographic effect forms a region with unique climatology.

Stretching to a length of 1490 km from Tapi Valley in the north to Kanyakumari in south it has an approximate area of 129037 km^2, it stretches to a width of 210 km in Tamilnadu and narrows to as small as 48 km in Maharashtra. The Ghats descend steeply to the coastal plains on the west, but merge rather gently through a series of hills with the Deccan plateau. Geologically the Ghats fall into two sections. The Western Ghats force the moisture laden winds coming off the Arabian Sea to rise and receive in consequence heavy precipitation of 2000 mm or more a year. To the lee of the Ghats is a region of rain shadow; and the eastern slopes of the Ghats are much drier than the Western face. The rainfall is heavier to the south and extends over 8–9 months a year; it is lower and restricted to 4 months of the south-west monsoon in the northern parts of the Western Ghats. The western slopes of the Ghats have a natural cover of evergreen forest, which changes to moist and then dry deciduous types as one comes to the eastern slopes. The vegetation reaches its highest diversity towards the southern tip in Kerala with its high statured, rich tropical rain forests.

At a time when the global interest is rising on the issue of the degenerating quality of the Ghat ecosystems and increasing crop failures in the agricultural tracts of the Ghats, the climatic processes of the region needs to be keenly observed. On a global outlook, Climate is one of the key aspects of the earth's environment. The climate system has continuously been modified and is being modified through natural processes and more recently, through human interferences. The atmospheric composition has been subjected to an evident change after the industrial revolution (Ruddiman, 2003). Anthropogenic activities like burning of fossil fuels, industrial emissions and deforestation have resulted in increased emissions and thereby increase in the atmospheric concentration of greenhouse gases like carbon dioxide, nitrous oxide and sulphur dioxide. These diatomic gases trap heat by selectively absorbing the outgoing long wave radiation, which increases the mean temperature of the atmosphere, a phenomenon known popularly as Global Warming.

Climate change has its impacts on all sectors of life such as agriculture and food security, water resources, human health, forests and biodiversity. Altered precipitation patterns, greater uncertainty in rainfall along with increased temperature are a consequence of the changes in climate, which has affected the planetary systems gravely. Anthropogenic influences have affected the global water cycle since 1960 and has contributed to observed increases in atmospheric moisture content in the atmosphere, to global-scale changes in precipitation patterns over land, to intensification of heavy precipitation over land regions and to changes in surface and sub-surface ocean salinity (IPCC, 2014). Changes in many extreme weather and climate events have been observed since about 1950. The total anthropogenic radiative force for 2011 relative to 1750 is 2.29 [1.13 to 3.33] W m^{-2} and it has increased more rapidly since 1970 than during prior decades. The total anthropogenic radiative force best estimate for 2011 is 43 per cent higher than that reported in AR4 for the year 2005. This is due to a combination of continued growth in most greenhouse gas concentrations and aerosols.

It is projected that extreme precipitation events over most of the mid-latitude land masses and over wet tropical regions will very likely become more intense and more frequent by the end of this century, as global mean surface temperature increases. Globally, it is likely that the area encompassed by monsoon systems will increase over the 21st century. Monsoon retreat dates will likely be delayed, resulting in lengthening of the monsoon season in many regions.

The studies conducted across the Western Ghats showed a decrease in the summer monsoon rainfall (Ghosh *et al.*, 2009) and an increase in hot days with subsequent decrease in cold nights over the region for the period from 1971 to 2005. Rajeevan *et al.* (2008) analysed the gridded rainfall data averaging 1803 stations over India and found an increase in the frequency of very heavy rainfall events (more than 150mm/ day) during post mid-1970s. Guhathakurta and Rajeevan (2008) has also reported an increase in rainfall during monsoon season over Konkan, Goa and Maharashtra region and a decrease over the Chhattisgarh and adjacent areas during 1901-2003.

The changing climate would have serious implications on all biotic and abiotic systems, threatening the very thread of life. The change in climate has become inevitable due to the present build up in radiative forcing and a scheme of mitigation may fall short. Adaptation and containing further forcing may pave the way ahead. This necessitates appropriate research on the current scenario, understanding of the temperature and precipitation dynamics associated with the changes in regional climate to build new strategies.

Keeping the above in view, the current study has been taken up with the objectives of analysing the trends in the Indian Summer Monsoon Rainfall over the Western Ghats emphasising specifically on precipitation extremes and visualizing the likely scenario in rainfall pattern.

CHAPTER 2

REVIEW OF LITERATURE

2.1 CLIMATE CHANGE AND RADIATIVE FORCING

The United Nations Framework Convention on Climate Change (UNFCCC) defines climate change as "a change of climate which is attributed directly or indirectly to human activity that alters the composition of the global atmosphere and which is in addition to natural climate variability observed over a comparable period" (Easterbrook, 2011). Human activities are responsible for the changes in the composition of the earth's surface and atmosphere. These directly influence the heat balance of the earth and thus act as drivers of the climate change. Radiative forcing is a measure of the net change in the earth's energy system in response to external perturbation, a positive radiative forcing indicates a warming trend while the negative radiative forcing indicates a cooling trend.

Radiative forcings can occur due to biotic processes, variations in solar radiation received by earth, plate tectonics, and volcanic eruptions. Human activities also enhance the climate change, often referred to as global warming. The global mean temperature has increased since 19^{th} century. In the period of 1901-2012, the combined sea and land surface temperature increased by 0.89^0 C, while the increase for the period 1950-2012 was 0.72^0 C. It is evident that, the maximum as well as minimum temperature over the land surface and sea surface has increased since 1950. Observations also show that the number of hot days and nights has increased while the cold days and night have decreased globally from 1951-2010. The extreme precipitation events have increased in many regions of the world. There has been a loss in Greenland and Antarctic ice sheets. Artic sea ice and the spring snow cover in the northern hemisphere has decreased in its extent and glaciers all over the world are shrinking (IPCC, 2014).

Human activities are in a great way responsible for the changes in the composition of the earth's surface and atmosphere. These directly influence the

heat energy of the earth and thus act as drivers to climate change. There is a 7.5 % increase in radiative forcing from GHGs from 2005 to 2011.The fourth IPCC report confirms the fact that more than half of increase in global mean temperature has been due to the anthropogenic activities from 1951 to 2010 (IPCC, 2013).

IPCC (2014), the latest in the assessment reports summarised the observed impacts of climate change in its Assessment Report 5 (AR5). Changes in the climate has consequences on all natural and human systems. Melting of ice and snow has altered hydrological systems and also affected the water resources in its quality and quantity. Many freshwater, terrestrial and marine species have shifted their seasonal activities, geographic ranges, migration patterns, abundance and there has been a drastic change in species interactions. Extreme weather events are on the rise and human livelihoods are affected as new diseases are emerging and those affected are usually the poverty stricken masses of developing countries.

It has been found that each of the last three decades has been successively warmer at the Earth's surface than any preceding decade since 1850. In the Northern Hemisphere, 1983–2012 was likely the warmest 30-year period during the last 1400 years. The globally averaged combined land and ocean surface temperature data calculated by a linear trend, has shown a warming of 0.85 [0.65 to 1.06] °C, through the period 1880 to 2012. When viewed on global scale, the ocean warming is largest near the surface, and the upper 75 m warmed by 0.11 [0.09 to 0.13] °C per decade over the period 1971 to 2010.The average rate of ice loss from glaciers around the world, excluding glaciers on the periphery of ice sheets was found to be at 226 [91 to 361] Gt yr^{-1} over the period 1971 to 2009, and very likely 275 [140 to 410] Gt yr^{-1} over the period 1993 to 2009. It is observed that the mean rate of global averaged sea level rise was 1.7 [1.5 to 1.9] mm yr^{-1} between 1901 and 2010, 2.0 [1.7 to 2.3] mm yr^{-1} between 1971 and 2010, and 3.2 [2.8 to 3.6] mm yr^{-1} between 1993 and 2010. The atmospheric concentrations of carbon dioxide, methane, and nitrous oxide have increased to levels unprecedented in at least the last 800,000 years. Carbon dioxide concentrations have increased by 40 per cent since pre-industrial times, primarily from fossil fuel emissions and

secondarily from net land use change emissions. The ocean has absorbed about 30 per cent of the emitted anthropogenic carbon dioxide, causing ocean acidification. The atmospheric concentrations of the greenhouse gases carbon dioxide (CO_2), methane (CH_4), and nitrous oxide (N_2O) have all increased since 1750 due to human activity. In 2011 the concentrations of these greenhouse gases were 391 ppm, 1803 ppb, and 324 ppb respectively and exceeded the pre-industrial levels by about 40, 150, and 20 per cent.

2.1.1 Radiative forcing (RF)

Natural and anthropogenic substances and processes that alter the earth's energy budget are drivers of climate change. Positive RF leads to surface warming, negative RF leads to surface cooling. Total radiative forcing is positive, and has over the years, led to an uptake of energy by the climate system. The largest contribution to total radiative forcing is caused by the increase in the atmospheric concentration of CO_2 since 1750. The total anthropogenic RF for 2011 relative to 1750 is 2.29 [1.13 to 3.33] W m^{-2}, and it has increased more rapidly since 1970 than during prior decades. The total anthropogenic RF estimate for 2011 is 43 per cent higher than that reported in AR4 for the year 2005. This is caused by a combination of continued growth in most greenhouse gas concentrations and improved estimates of RF by aerosols indicating a weaker net cooling effect. The RF from emissions of well-mixed greenhouse gases (CO_2, CH_4, N_2O, and Halocarbons) for 2011 relative to 1750 is 3.00 [2.22 to 3.78] W m^{-2}). The RF from changes in concentrations in these gases is 2.83 [2.26 to 3.40] W m^{-2}.

2.2 INDIAN SUMMER MONSOON RAINFALL

At the most basic level, the seasonal cycle of solar heating through boreal spring warms the land regions surrounding South and Southeast Asia faster than the adjoining oceans, owing to differences in heat capacity, and develops a large-scale meridional surface temperature gradient. This results in the formation of a surface heat low over northern India in late spring; the north–south pressure gradient then induces a cross-equatorial surface flow and return flow aloft (Li and

Yanai, 1996). The dynamics and thermodynamics of the South Asian monsoon go beyond this simple land–sea breeze argument.

The Himalaya and Tibetan Plateau ensure that sensible heating during boreal spring occurs aloft, meaning that the large-scale meridional temperature gradient exists not just at the surface but over significant depth in the troposphere, anchoring the monsoon onset and intensity (Fasullo and Webster, 2003; Chou, 2003).

The intense solar heating in late spring and summer gives thermodynamic conditions favouring the occurrence of convection poleward of the Equator, allowing the monsoon to be viewed as a seasonal migration of the Intertropical Convergence Zone (ITCZ) (Prive and Plumb, 2007).

The north–northwest migration of boreal winter convection from the equatorial region and its interaction with circulation leads to a positive feedback and deeper monsoon trough, enhancing the cross-equatorial flow in the lower troposphere that feeds moisture to the monsoon, as well as the Tibetan anticyclone and easterly jet with a return cross-equatorial flow at upper levels (Meehl, 1987) and Webster *et al.,* 1998).

The north–south-oriented East African Highlands anchor the low-level cross equatorial flow and the Earth's rotation aids in the formation of the low-level westerly jet as it approaches South Asia from across the Arabian Sea (Findlater, 1969; Boos and Emanuel, 2009).

The rapid intensification of rainfall and circulation during the onset can be attributed to wind–evaporation feedback as well as feedbacks between extratropical eddies and the tropical circulation (Bordoni and Schneider, 2008).

Rossby-wave interactions in conjunction with a warmer sea surface temperature (SST) over the Bay of Bengal (Hoskins and Rodwell 1996: Shenoi *et al.,* 2002) help to set up an east/west asymmetry of wet/dry precipitation in the South Asia monsoon region. In addition, the Himalayas act as a mechanical barrier in preventing the advection of dry air to South (Boos and Kuang, 2010). Further

local details of the precipitation distribution are fixed by the Western Ghats mountains on the west coast of India and mesoscale convective systems embedded into the monsoon trough contribute a large proportion of rainfall over north-eastern peninsular India. The Indian Ocean also plays a regulatory role in the monsoon owing to the seasonality of meridional oceanic heat transports, themselves related to the seasonal monsoon winds (Loschnigg and Webster, 2000). Thus it can be inferred that the South Asian monsoon as a fully coupled ocean–land–atmosphere system that is also influenced by fixed orography. However, many of the above mechanisms, including all the coupled feedbacks involved, are yet to be fully explored in comprehensive non-linear general circulation models (GCM).

The familiar pattern of seasonally reversing winds transports moisture from over the warm Indian Ocean and ultimately contributes 80 per cent of annual rainfall to South Asia between June and September.

The monsoon undergoes seasonal changes in response to slow variations at the lower boundary of the atmosphere (Charney and Shukla, 1981) including the El Niño/Southern Oscillation (ENSO) or snow cover. However, these inter-annual variations in rainfall are relatively low, the inter annual standard deviation being around 10 per cent of the summer rainfall total. It is the active or break events on short (intra--seasonal) timescales of a few days to weeks that often have large impacts that particularly affect agriculture or water supply (Webster *et.al.*, 1998) . These include the famous break of July 2002, where less than 50% of the usual rainfall fell , contributing to substantially reduced agricultural output and growth of gross domestic product (Subbiah, 2002). Understanding how variability in the South Asian monsoon on daily to inter-annual timescales will change against a background of anthropogenic warming is a demanding task.

2.3 WESTERN GHATS

The Western Ghats, the mountain range that runs parallel to the western coast of the Indian peninsula is a UNESCO World Heritage Site and is one of the eight " hotspots" of biological diversity in the world. The range runs north to south

along the western edge of the Deccan Plateau, and separates the plateau from a narrow coastal plain, called Konkan, along the Arabian Sea. A total of thirty nine properties including national parks, wildlife sanctuaries and reserve forests were designated as world heritage sites. The area has over 7402 species of flowering plants, 1814 species of non-flowering plants, 139 mammal species, 508 bird species, 179 amphibian species, 6000 insects species and 290 freshwater fish species. At least 325 globally threatened species occur in the Western Ghats.

Climate in the Western Ghats varies with altitudinal gradation and distance from the equator. The climate is humid and tropical in the lower reaches tempered by the proximity to the sea. Elevations of 1,500 m and above in the north and 2000 m and above in the south have a more temperate climate. Average annual temperature is around 15 °C. At some parts frost is common, and temperatures touch the freezing point during winter months. Mean temperature range from 20 °C in the south to 24 °C in the north. It has also been observed that the coldest periods in the South Western Ghats coincide with the wettest.

During the monsoon season between June and September, the unbroken Western Ghats chain acts as a barrier to the moisture laden clouds. The heavy, eastward-moving rain-bearing clouds are forced to rise and in the process deposit most of their rain on the windward side. Rainfall in this region averages 3000–4000 mm with localized extremes touching 9000 mm. The eastern region of the Western Ghats which lie in the rain shadow, receive far less rainfall averaging about 1000 mm bringing the average rainfall figure to 2,500 mm. Data from rainfall figures reveal that there is no relationship between the total amount of rain received and the spread of the area. Some areas to the north in Maharashtra while receiving heavier rainfall are followed by long dry spells, while regions closer to the equator receiving less annual rainfall, have rain spells lasting almost the entire year.

Jha *et.al.*, 2000 estimated changes in forest cover between 1973 and 1995 in the southern part of the Western Ghats using satellite data. The study area of approximately 40 000 km^2 showed a loss of 25.6 per cent in forest cover over 22

years. The dense forest was reduced by 19.5 per cent and open forest decreased by 33.2 per cent. As a consequence, degraded forest increased by 26.64 per cent. There has been a great deal of spatial variability in the pattern of forest loss and land use change throughout the region.

2.3.1 Orographic Effect of Western Ghats

A study conducted by Rajendran *et.al.*, 2012 suggests that the summer mean rainfall and the vertical velocities over the orographic regions of Western Ghats have significantly weakened during the recent decades. They found that by the end of the twenty-first century, reduced orographic precipitation over the narrow Western Ghats south of 16°N would occur found to be associated with drastic reduction in the south-westerly winds and moisture transport into the region, weakening of the summer mean meridional circulation and diminished vertical velocities. It is inferred to be due to larger upper tropospheric warming relative to the surface and lower levels, which decreases the lapse rate causing an increase in vertical moist static stability (which in turn inhibits vertical ascent) in response to global warming. Increased stability that weakens vertical velocities leads to reduction in largescale precipitation which is found to be the major contributor to summer mean rainfall over WG orographic region. This is further supported by a significant decrease in the frequency of moderate-to-heavy rainfall days over WG which is a typical manifestation of the decrease in large-scale precipitation over this region.

When the long-term changes in the summer monsoon rainfall over the west coast of India and adjoining eastern Arabian Sea (WCA) were investigated using the gauge-adjusted multi-satellite rainfall data for the period 1979–2010 , it was found that the region receives maximum rainfall during the peak monsoon months of July and August. The time series of peak monsoon rainfall averaged over the maximum rainfall decrease region bounded by 10–20°N and 72–77° E showed a decreasing trend during the study period (Prakash *et al.*, 2013). The rainfall averaged over the WCA showed a significant upward trend since 2002 which

suggests the need for further analysis using longer period of satellite-based rainfall data to better understand the long-term changes in the summer monsoon rainfall over this region.

To understand the inter-seasonal and inter-annual patterns rainfall over Agumbe – popularly known as the Cheerapunji of the South India, a research conducted by Manjunatha *et al.*, (2015) for the years 1963-2010 revealed that seasonally, the maximum amount in rainfall occurs during the summer followed by fall, spring and the least during winter (84.31 to 98.98%, 0 to 9.92%, 0 to 8.23% and 0 to 0.41% respectively). Though the rainfall of the study area is generally in phase with that of all India summer rainfall, there was an increasing trend of both inter-annual and seasonal rainfall suggesting the induction of global warming in supplying moisture from the Indian Ocean. The rate of increase has been found to be maximum during the summer, followed by spring and fall seasons with a pronounced increasing in the annual rainfall (22.85, 4.29, 2.82 and 28.58 mm yr^{-1} respectively). Generally, the annual lows and highs are generally in agreement with El Niño and La Niña years respectively. Despite increasing in rainfall, the major part of the study area suffers from the shortage of water resource particularly during the spring season suggesting for a better management of the water resource in high rainfall terrain (Rajeevan *et al.*, 2005; Shepard, 1968).

2.4 RAINFALL TREND ANALYSIS

Parthasarathy and Dhar (1974) found that the annual rainfall for the period 1901–1960 had a positive trend over Central India and the adjoining parts of the peninsula, and a decreasing trend over some parts of eastern India.

Pant and Hingane (1988) found an increasing trend in mean annual and SW monsoon rainfall over meteorological sub-divisions of Punjab, Haryana, west Rajasthan, east Rajasthan and west Madhya Pradesh during the period 1901–1982.

Kumar *et al.*, (1992) reported that, northeast peninsula, northeast India and northwest peninsula experienced a decreasing trend (ranged between 6% and 8% of the normal per 100 years) in the monsoon rainfall. But the west coast, central

peninsula and northwest India experienced increasing trend (about 10–12% of the normal per 100 years) in monsoon rainfall.

Singh and Sontakke (2002) analysed rainfall data for the period 1829–1999 over the Indo-Gangetic Plains (IGP) and found a significant increasing trend (170 mm per100 years) from 1900 in the summer monsoon rainfall over western IGP; non-significant decreasing trend (5 mm per100 years) from 1939 over central IGP and non-significant decreasing trend (50 mm per100 years) during 1900–1984 and non-significant increasing trend (480 mm per100 years) during 1984–1999 over eastern IGP.

Ramesh and Goswami (2007) analysed the daily gridded observed rainfall data for the period 1951–2003 and found a decreasing trends in both early and late monsoon rainfall and number of rainy days over India. Analysis of rainfall amount during different seasons indicated decreasing tendency in the summer monsoon rainfall over the Indian land mass and increasing trend in the rainfall during pre-monsoon and post-monsoon months.

Kumar and Jain (2010) conducted a trend analysis of rainfall data of 135 years (1871– 2005). The results indicated no significant trend for annual, seasonal and monthly rainfall on an all-India basis. Annual and monsoon rainfall decreased, and pre-monsoon, post monsoon and winter rainfall increased over the years, with maximum increase in the pre-monsoon season. Monsoon months of June, July and September witnessed decreasing rainfall, whereas August showed increasing trend on an all-India basis. Further analysis on sub divisional basis (30 sub-divisions) indicated that half of them have increasing trend in annual rainfall, but for only three sub-divisions, namely Haryana, Punjab and coastal Karnataka, this trend was statistically significant. Only the Chhattisgarh sub-division had significant decreasing trend out of the 15 sub-divisions showing decreasing trend in annual rainfall. All the five regions showed nonsignificant trend in annual, seasonal and monthly rainfall for most of the months.

Kumar *et al.*, (2010) conducted an analysis of rainfall data at five stations (Srinagar, Kulgam, Handwara, Qazigund and Kukarnag) in the Kashmir Valley for the period 1903–1982. The results showed that the first three stations experienced a decreasing trend in annual rainfall; the largest decrease was for Kulgam (20.16% of mean per100 years) and the smallest for Srinagar. The decreasing trend in winter rainfall was statistically significant (95% confidence level) at Kulgam and Handwara, whereas none of the increasing trends in the pre-monsoon and post-monsoon season was significant. Srinagar and Handwara witnessed a decreasing (nonsignificant) trend in annual rainy days, whereas Kulgam experienced the opposite trend. All the stations experienced a decreasing trend in monsoon and winter rainy days. Qazigund and Kukarnag experienced decreasing annual rainfall, whereas Srinagar showed increasing annual rainfall during 1962–2002. Annual, pre-monsoon, post-monsoon and winter rainfall increased (nonsignificant), whereas monsoon rainfall decreased (nonsignificant) at Srinagar during the last century.

Pal and Al-Tabbaa (2011) analysed the seasonal precipitation trends in India using parametric and non-parametric statistical techniques. Significant trends were not found in annual or seasonal precipitation amount in the period of 1871–2005 in various regions in India; however, significant changes were observed for the period of 1954–2003. In all cases, all the regions are showing trends either positive or negative. Precipitation has an increasing tendency in the winter and autumn seasons whereas a decreasing tendency in spring and monsoon seasons in Kerala. These seasonal changes of rainfall in India could be due to either or the cumulative effect of multiple actors, namely the changes in the number of rainy days, rainfall intensity and extremes, sea surface temperature changes, convective phenomena and ENSO. A great difference in change in spatial rainfall patterns were noticed in the results attributed to a change in regional circulation pattern for tremendous spatial inhomogeneity in the trends in surface temperature over India or the oceans or both. Therefore, even if all-India monsoon rainfall decreased, the geographical coverage at various spatial scales those also receive monsoon rainfall might not have changed significantly.

Subash *et al.*, (2011) conducted an investigation on the observational characteristics of rainfall and temperature in Central Northeast India (CNE India), using Mann–Kendall non-parametric test. The long-term (1889–2008) mean annual rainfall of CNE India was found to be 1,195.1 mm with a standard deviation of 134.1 mm and coefficient of variation of 11 per cent. A significant decreasing trend of 4.6 mm per year for Jharkhand and 3.2 mm per day for CNE India was found. Since rice crop is the important kharif crop (May– October) in this region, the decreasing trend of rainfall during the month of July may delay/affect the transplanting/vegetative phase of the crop, and assured irrigation is very much needed to tackle the drought situation. During the month of December, all the meteorological subdivisions except Jharkhand were found to exhibit a significant decreasing trend of rainfall during recent period. The decrease of rainfall during December may hamper sowing of wheat, which is an important Rabi crop (November–March) in most parts of this region. Maximum temperature shows significant rising trend of 0.008°C per year during monsoon season and 0.014°C per year during post-monsoon season during the period 1914– 2003. The annual maximum temperature also shows significant increasing trend of 0.008°C per year during the same period. Minimum temperature shows significant rising trend of 0.012°C per year during post monsoon season and significant falling trend of 0.002°C per year during monsoon season. A significant 4– 8 years peak periodicity band has been noticed during September over Western UP, and 30–34 years periodicity has been observed during July over Bihar subdivision. However, as far as CNE India is concerned, no significant periodicity has been noticed in any of the time series.

Subash and Sikka (2014) conducted a study to investigate the trends in rainfall and temperature. They found that, annual maximum temperature showed an increasing trend in all the homogeneous temperature regions and that corresponding annual rainfall also follow the same pattern in all the regions, except North East. In monthly analysis, no definite pattern had been observed between trends in maximum and minimum temperature and rainfall, except during October. Increasing trends of maximum and minimum temperature during October

accelerate the water vapour demand and most of the lakes, rivers, ponds and other water bodies with no limitation of water availability during this time fulfils the water vapour demand and shows an increasing trend of rainfall activity. This study revealed that, there exists no direct relationship between increasing rainfall and increasing maximum temperature when monthly or seasonal pattern is concerned over meteorological subdivisions of India.

Thomas *et al.*, (2015) analysed the trends in the one day maximum rainfall series over Narmada basin and a significant positive trend at 95 per cent significance level was found. An increasing trend in the magnitude of 1-day maximum rainfall over the basin was found with more areas in the basin experiencing high intensity storms, which was more prominent in the most recent 20 years. Drought duration estimated by the standardized precipitation index for the periods 1951–1970 and 1989–2008 indicated that the entire basin has experienced frequent droughts during the recent two decades, with the middle zone of the basin being more prone to droughts.

2.5 RETURN PERIOD ANALYSIS

Rainfall data may be analysed in different ways depending on the problem under consideration. For instance, analysis of consecutive days' maximum rainfall is more relevant for drainage design of agricultural lands (Bhattacharya and Sarkar, 1982; Upadhaya and Singh, 1998), whereas analysis of weekly rainfall data is more useful for planning cropping pattern and its management. Engineering and hydrologic design considerations have always relied on analyses of extreme-rainfall return intervals.

The analysis of rainfall data deals with interpreting past record of rainfall events in terms of future probabilities of occurrence. The analysis of rainfall data for computing expected rainfall of a given frequency is commonly done by utilizing different probability distributions.

Heavy-rainfall events have become more frequent since the middle of the last century in many regions across the globe (Suppiah and Hennessy, 1998). In

some cases, the extremes have changed despite decreases or flat trends in mean rainfall (Groisman *et al.*, 1999; Goswami *et al.*, 2006). These changes have been seen both at the daily and sub daily scales.

Simulations using coupled atmosphere ocean general circulation models (GCM) also indicate increases in the frequency and/or intensity of extreme rainfall events. Kharin and Zwiers (2000) showed that changes in extreme precipitation can be expected across the globe and that the relative change in extreme precipitation amounts can be expected to be larger than the change in mean precipitation. They base their findings on transient simulations from the Canadian Centre for Climate Modelling and Analysis global model.

Frequency analysis of rainfall data had been done for different places in India (Jeevrathnam and Kumar, 1979; Sharda and Bhushan, 1985; Singh, 2001).

Bhaskar *et al.*, (2006) did frequency analysis of consecutive days' peak rainfall at Banswara, Rajasthan and found gamma distribution as the best fit as compared to other methods of probability fitting after due testing with Chi-square value.

Kwaku and Duke (2007) revealed that the log-normal distribution was the best fit probability distribution tool for analysing five consecutive days' maximum rainfall in respect of Accra, Ghana.

CHAPTER 3

MATERIALS AND METHODS

The objective of this research was to study the temporal and spatial distribution of Indian summer (South-West) Monsoon Rainfall (ISMR) over the area enclosing the Western Ghats and up to the coastline. The procedure adopted for the analysis of Indian summer monsoon is outlined in this section.

3.1 DATA AND TOOLS USED

Data and tools used for the current study are described in the following sections.

3.1.1 Area of Study

The Western Ghats is a chain of highlands running along the western edge of the India subcontinent, from the states Maharashtra, Goa, Karnataka and Kerala. The study is focused on region experiencing orographic rainfall bounded between latitude 8° to 21° N and longitude 70° to 78° E. The study area is illustrated in Figure 1. It has been observed from DEM (Digital Elevation Model) data that the WG runs parallel to West coast of India 50 km away on an average from shore line. WG extends about 1600 km (North-south) in length and 100 km (East-West) in width. The average elevation of WG is approximately 800 m with some apexes rising more than 2000 m in elevation.

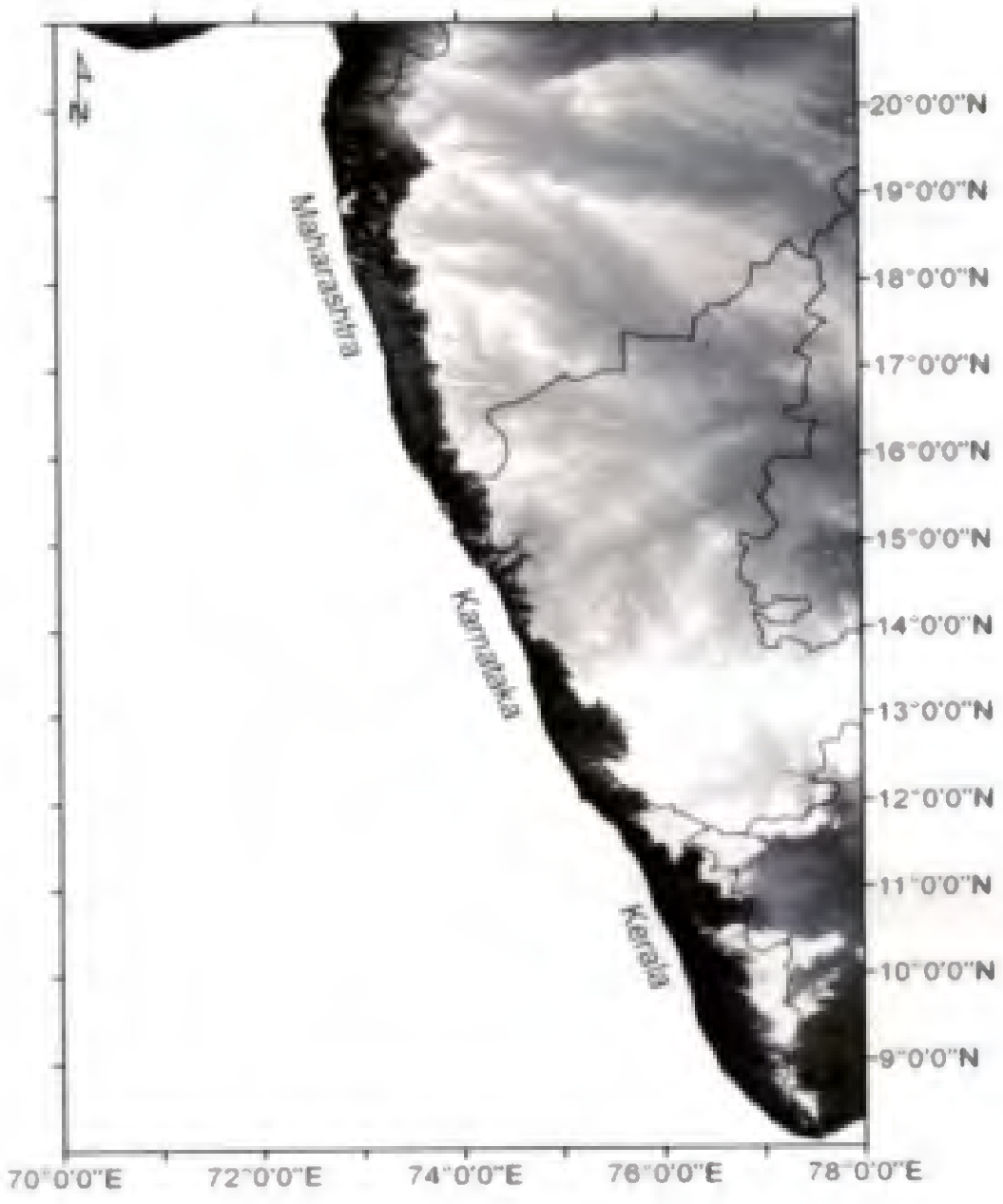

Figure 1. Study area

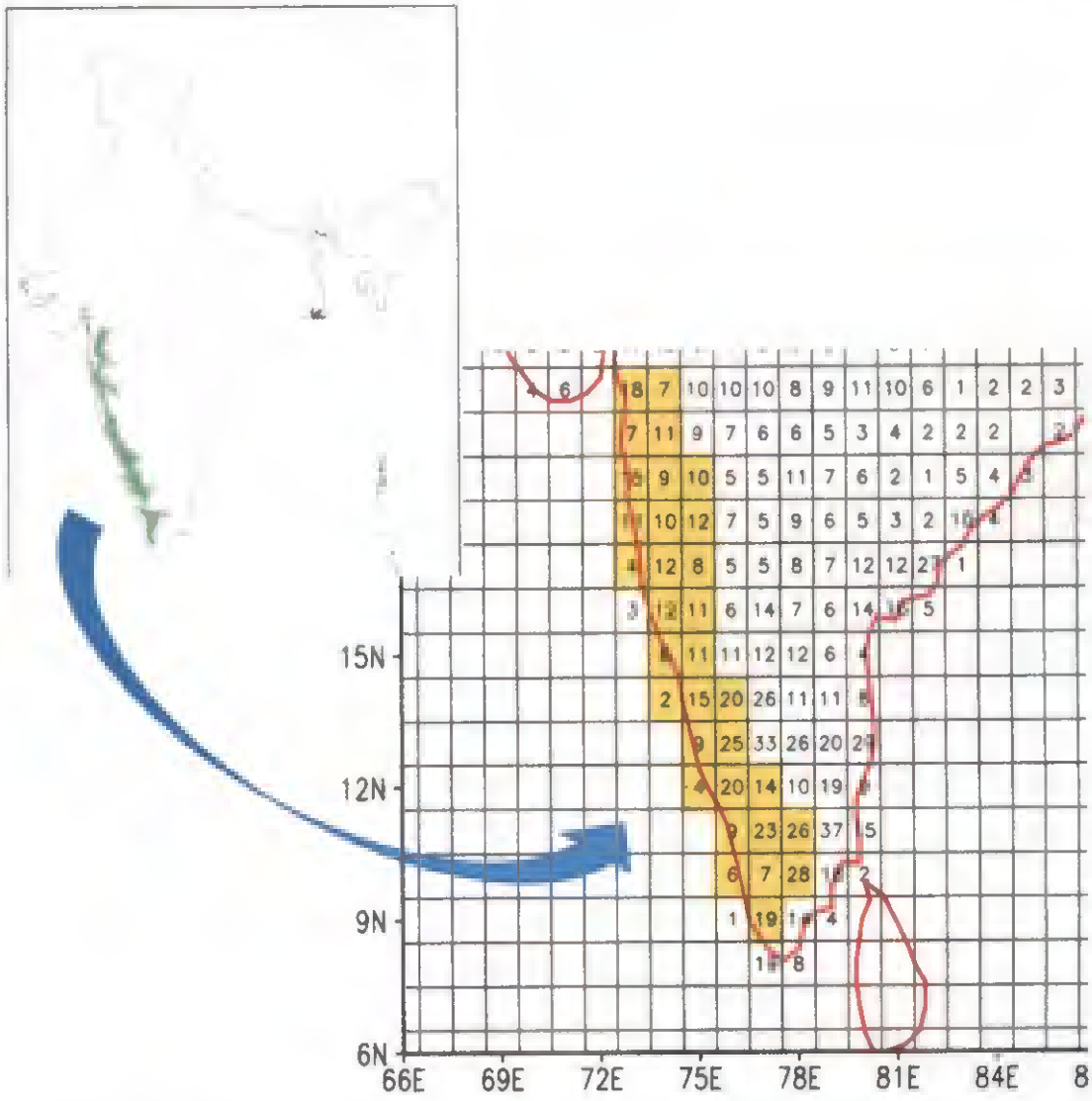

Figure 2. The data grids under the area of research (Rajeevan *et al.*, 2006)

3.1.2 Data utilized

The $1^0 \times 1^0$ daily gridded rainfall data prepared by the India Meteorological Department (IMD) for the Indian land mass (6.5WN–38.5WN and 66.5WE–100.5WE) has been used in the present study (Rajeevan *et al.*, 2006). IMD has the rainfall records of 6329 stations with varying periods. Out of these, 537 are IMD observatory stations, 522 are under the Hydrometeorology programme and 70 are Agro met stations. The remaining are rainfall-reporting stations maintained by state governments. However, only 1803 out of 6329 stations had a minimum 90 percent data availability during the analysis period. Only 1803 stations were taken in order to minimize the risk of generating temporal inhomogeneities in the gridded data due to varying station densities. The density of stations is not uniform throughout the country. Density is the highest over south peninsula and poor over northern plains of India (Uttar Pradesh, for example) and eastern parts of Central India. On an average, 1600 station data were available for the analysis. However, after 1995, the number of stations available for analysis dropped significantly. This is due to the delay in digitizing and archiving the manuscripts which are received at IMD in a delayed mode.

The data interpolation technique used for the dataset was Shepard's method (Shepard, 1968). In this method, interpolated values are computed from a weighted sum of the observations. Given a grid point, the search distance is defined as the distance from this point to a given station. The interpolation is restricted to the radius of influence. For search distances equal to or greater than the radius of influence, the grid point value is assigned a missing code when there is no station located within this distance. In this method, interpolation is limited to the radius of influence. A predetermined maximum value limits the number of data points used which, in the case of high data density, reduces the effective radius of influence. The method proposed by Shepard to locally modify the scheme for including the directional effects and barriers is also considered. In this interpolation method, no initial guess is required. Out of the all India time series data, only 32 grids

constitute the current scope of this research. The grids are represented in Table 1. The grids are indexed and named based on the index given by IMD.

Table 1. Constituent grids of the study area

Coordinates	Index	Coordinates	Index
9N 77E	Grid 81	15N 75E	Grid 289
10N 76E	Grid 115	16N 74E	Grid 323
10N 77E	Grid 116	16N 75E	Grid 324
10N 78E	Grid 117	17N 73E	Grid 357
11N 76E	Grid 150	17N 74E	Grid 358
11N 77E	Grid 151	17N 75E	Grid 359
11N 78E	Grid 152	18N 73E	Grid 392
12N 75E	Grid 184	18N 74E	Grid 393
12N 76E	Grid 185	18N 75E	Grid 394
12N 77E	Grid 186	19N 73E	Grid 427
13N 75E	Grid 219	19N 74E	Grid 428
13N 76E	Grid 220	19N 75E	Grid 429
14N 74E	Grid 253	20N 73E	Grid 462
14N 75E	Grid 254	20N 74E	Grid 463
14N 76E	Grid 255	21N 73E	Grid 497
15N 74E	Grid 288	21N 74E	Grid 498

3.1.3 Tools used

Matlab 2016, Microsoft Excel, Xlstat and Easyfit were used for calculation purposes and Statistical analyses in the current study.

3.2 RAINFALL TREND ANALYSIS

The trends of extreme events in rainfall in terms of one day maximum rainfall, heavy, very heavy and extreme events, shift of dates of one day maximum rainfall and contribution of heavy and moderate events to the ISMR over the time period of study is analysed. The Return Levels for the Return Periods of 2, 5, 10, 25, 50 and 100 years are also calculated

3.2.1 One day maximum rainfall

One day maximum rainfall is the maximum rainfall obtained on a single day in a given year. Here, the maximum rainfall in the monsoon season is taken i.e., the maximum magnitude of rainfall which is received in the months of June, July, August and September. A time series of annual maximum rainfall is thus extracted out of the whole time series (1951-2008) and trends are calculated for both the grids and for the whole study area. A latitude wise analysis is also carried out. For this study, the widely used modified Mann-Kendall test was run at 5 percent significance level on time series data which is a non-parametric method of trend analysis. The annual maximum rainfall can be used as a flood indicator in the various parts of the region.

3.2.1.1 Mann Kendall method

A trend refers to an association or correlation. An estimate of the degree to which two sets of variables vary together, with no distinction between dependent and independent variables between concentration and time or spatial location. Trends take various forms, such as increasing, decreasing, or periodic.

Mann Kendall test is a statistical test widely used for the analysis of trend in climatologic and in hydrologic time series (Yue and Wang, 2004). There are two advantages of using this test. First, it is a non-parametric test and does not require the data to be normally distributed. Second, the test has low sensitivity to abrupt breaks due to inhomogeneous time series. Any data reported as non-detects are included by assigning them a common value that is smaller than the smallest measured value in the data set. According to this test, the null hypothesis H0 assumes that there is no trend (the data is independent and randomly ordered) and this is tested against the alternative hypothesis H1, which assumes that there is a trend (Onoz and Bayazit, 2012).

The computational procedure for the Mann Kendall test considers the time series of n data points and Ti and Tj as two subsets of data where,

i = 1,2,3,…, n-1 and

j = i+1, i+2, i+3, …, n.

The data values are evaluated as an ordered time series. Each data value is compared with all subsequent data values. If a data value from a later time period is higher than a data value from an earlier time period, the statistic *S* is incremented by 1. On the other hand, if the data value from a later time period is lower than a data value sampled earlier, *S* is decremented by 1. The net result of all such increments and decrements yields the final value of *S*. The Mann-Kendall S Statistic is computed as follows:

$$S = \sum_{i=1}^{n-1} \sum_{j=i+1}^{n} sign\,(Tj - Ti)$$

$$Sign\,(Tj - Ti) = \begin{cases} 1\ if\ Tj - Ti > 0 \\ 0\ if\ Tj - Ti = 0 \\ -1\ if\ Tj - Ti < 0 \end{cases}$$

where, Tj and Ti are the annual values in years j and i, j > i, respectively.

If n < 10, the value of |S| is compared directly to the theoretical distribution of S derived by Mann and Kendall. The two tailed test is used. At certain probability level H0 is rejected in favour of H1 if the absolute value of S equals or exceeds a specified value Sα/2, where Sα/2 is the smallest S which has the probability less than α/2 to appear in case of no trend. A positive (negative) value of S indicates an upward (downward) trend. For n ≥ 10, the statistic *S* is approximately normally distributed with the mean and variance as follows:

$$E(S) = 0$$

The variance (σ^2) for the S-statistic is defined by:

$$\sigma^2 = \frac{n(n-1)(2n+5) - \Sigma\ ti\ (i)(i-1)(2i+5)}{18}$$

In which ti denotes the number of ties to extent i. The summation term in the numerator is used only if the data series contains tied values.

The standard test statistic Zs is calculated as follows:

$$Zs = \begin{cases} \frac{s-1}{\sigma} \; for \; S > 0 \\ 0 \; for \; S = 0 \\ \frac{s+1}{\sigma} \; for \; S < 0 \end{cases}$$

The test statistic Zs is used a measure of significance of trend. In fact, this test statistic is used to test the null hypothesis, H0. If | Zs| is greater than Zα/2, where α represents the chosen significance level (eg: 5% with Z 0.025 = 1.96) then the null hypothesis is invalid implying that the trend is significant.

Another statistic obtained on running the Mann-Kendall test is Kendall's tau, which is a measure of correlation and therefore measures the strength of the relationship between the two variables. Kendall's tau, like Spearman's rank correlation, is carried out on the ranks of the data. That is, for each variable separately, the values are put in order and numbered, 1 for the lowest value, 2 for the next lowest and so on. In common with other measures of correlation, Kendall's tau will take values between ±1 and +1, with a positive correlation indicating that the ranks of both variables increase together whilst a negative correlation indicates that as the rank of one variable increases, the other decreases. In time series analysis it is essential to consider autocorrelation or serial correlation, defined as the correlation of a variable with itself over successive time intervals, prior to testing for trends. Autocorrelation increases the chances of detecting significant trends even if they are absent and vice versa. In order to consider the effect of autocorrelation, Hamed and Rao (1998) suggested a modified Mann-Kendall test, which calculates the autocorrelation between the ranks of the data after removing the apparent trend. The adjusted variance is given by:

$$Var\,[S] = \frac{1}{18}[N(N-1)(2N+5)]\frac{N}{NS^*}$$

Where,

$$\frac{N}{NS^*} = 1 + \frac{2}{N(N-1)(N-2)} \sum_{i=1}^{p} (N-i)(N-i-1)(N-i-2) p_{s(i)}$$

Where, N is the number of observations in the sample, NS* is the effective number of observations to account for autocorrelation in the data, p_s (i) is the autocorrelation between ranks of the observations for lag i, and p is the maximum time lag under consideration.

Software used for performing the statistical Mann-Kendall test is Addinsoft's XLSTAT 2014. The null hypothesis is tested at 5% confidence level for both the Western Ghats region and the constituent grids. In addition, to compare the results obtained from the Mann-Kendall test, linear trend lines are plotted for each grid using Microsoft Excel 2016.

3.2.2 Shift of dates

The shift in dates of the occurrence of the annual maximum rainfall (ODMR) of the summer monsoon season for the study area is found out and plotted on a histogram. The significance of the shift is also calculated.

3.2.3 Change in frequency of high intensity rainfall

Based on the total rainfall received in any given day, the rainfall events have been classified into various categories. Often, a percentile based threshold is used for defining extremes in area with wide climatological variability but a fixed threshold approach is used in the current study over Western Ghats as it gives a fair amount of idea on the change in specific rainfall magnitudes over the region. Different threshold values have been used by various researchers (Stephenson *et al.*, 1999; Sen and Balling 2004 and Goswami *et al.*, 2006) for classifying the rainfall. This study considers the threshold values as follows: extreme rainfall (>200 mm/ day); very heavy rainfall (>150 mm/day); and heavy rainfall (>100 mm/day). A day that receives rainfall less than 2.5 mm has been considered to be

a dry day. The major focus being to analyse the extreme events, rainfall between 2.5 and 100 mm on one day has been considered as a moderate event. Time series for each of the above categorization has been prepared from the available gridded data for further analysis. The change in frequency of high intensity rainfall in terms of its distribution and occurrence frequency are found and trends are analysed. Trends are checked for both the complete time period and for the initial and final 20 year periods in the data series. The split series are 1951–1970 and 1989–2008. The data during 1971–1988 was deselected to understand the contrast in the trend in extreme events during the two distinct time periods 1951–1970 (past) and 1989–2008 (present). The latter period may represent the changes that have occurred to the regional rainfall in the last few decades in the changing climate scenario.

3.2.3.1 Temporal distribution of high intensity rainfalls.

In order to investigate whether more areas in the basin have experienced high intensity rainfalls in recent years (change in spatial variability), temporal distribution of high intensity rainfall for different grids, have been analysed. The number of grids getting rainfall events of heavy, very heavy, and extreme magnitudes as mentioned above through the years are calculated.

3.2.3.2 Occurrence frequency of high intensity rainfalls

Occurrence frequency reflects the number of occurrences or instances of heavy, very heavy and extreme events on a single day over the time period. The trends are analysed for significance using Mann Kendall method.

3.2.4 Contribution of moderate and high intensity rainfall events to the ISMR mean

Moderate events (>2.5 mm and < 100 mm) and high intensity rainfall events (>100mm) on a single day are extracted and percentage analysis is done to ascertain the contribution of these events to the total summer monsoonal rainfall. This is done for all the grids and for the whole region for each year. Split time series of 1951-1970 and 1989-2008 is taken to calculate the total percentage contribution.

3.3 RETURN PERIOD ANALYSIS

The intense precipitation events have caused a major impact on the socioeconomic activities of the Western Ghats, making the population vulnerable to the behaviour and variability of the climate system. Many incidents of extreme rainfall in the region has caused serious calamity in this region, for instance the landslides that occur in the upland regions and the reservoirs which overflow in summer monsoon during high intensity rainfalls causing damage to life.. In this context, the probabilistic prediction of occurrence of extreme precipitation events is of vital importance for the planning of activities exposed to its adverse effects. One way to model these events is use the extreme values theory (EVT), through the generalized extreme value (GEV) distribution, which includes the distributions of Gumbel, Fréchet, and Weibull distributions.

The return period is defined by Bedient and Huber (1948), as an annual maximum event that has a return period (or recurrence interval) of T years, if this value is equalled or exceeded once, on the average, every T years. The reciprocal of T is called the probability of the event or the probability the event is equalled or exceeded in any one year. The function below shows this relationship.

$$P = 1/T$$

There are numerous methods to estimate precipitation, probabilities and return periods, which have been proposed for the plotting of precipitation data. Texts of hydrology call those plotting position formulas, probability plots and goodness-of-fit tests.

In this study, synthetic series of precipitation were used, which consists in using the daily maximum values of each region, i.e., the synthetic series was formed by data from different stations for different days. The synthetic series were analysed considering the EVT, which is a branch of theoretical probability that studies the stochastic behaviour of the extremes associated to a distribution function F, normally unknown. This theory deals essentially with the asymptotic distributional behaviour of two types of data, namely, the so-called block maxima

and peaks over threshold. The first type refers to the maximum values extracted from blocks (subsets) of observations, whereas the second type refers to observations that exceed a given threshold. The block maxima approach is used here, i.e., annual maximum or one day maximum rainfall from every year in the data time series is taken as the extreme event.

3.3.1 Extreme Value Theory

Coles (2001) demonstrates the initial formulation of the model as follows:

$$M_n = \max\{x_1, \ldots x_n\}$$

where M_n is the maximum of n units, and $x1, \ldots, xn$ a sequence of independent random variables identically distributed with cumulative distribution F in common. The exact distribution function of the maximum can be obtained for all values of n, as follows:

$$F_{M_n(x)} = P(M_n \leq x) = P(X_1 \leq x, \ldots, X_n \leq x) = (F_x(x))^n$$

Since F is unknown, a way of knowing it is to seek families of models next in the Fn. distributions. The idea is similar to the approach procedure of the distribution of sample means in normal distribution, according to the central limit theorem. Moreover, the central limit theorem provides a unique limit of distribution, while EVT includes three different families of asymptotic distributions. Its main goal is to stimulate the upper tail of a probability distribution function of a set of independent and identically distributed observations.

3.3.2 Runs test

To test the hypothesis of independence of data, the nonparametric test of sequences of adherence to the normal distribution, called runs tests, which checks whether the elements of the series are independent of each other was used. A 5 per cent significance level was adopted for the test.

The runs test can be used to decide if a data set is from a random process. A run is defined as a series of increasing values or a series of decreasing values.

The number of increasing, or decreasing, values is the length of the run. In a random data set, the probability that the $(I+1)^{th}$ value is larger or smaller than the I^{th} value follows a binomial distribution, which forms the basis of the runs test. The first step in the runs test is to count the number of runs in the data sequence. Values above the median are coded as positive and values below the median as negative.

A run is defined as a series of consecutive positive (or negative) values.

The runs test is defined as:

H0: the sequence was produced in a random manner.

H1: the sequence was not produced in a random manner.

The test statistic is:

$$Z = \frac{R - \bar{R}}{S_R}$$

where R is the observed number of runs, $\bar{R}$, is the expected number of runs, and sR is the standard deviation of the number of runs. The values of $\bar{R}$ and sR are computed as follows:

$$\bar{R} = \frac{2n_1 n_2}{n_1 + n_2} + 1$$

$$s_R^2 = \frac{2n_1 n_2 (2n_1 n_2 - n_1 - n_2)}{(n_1 + n_2)^2 (n_1 + n_2 - 1)}$$

with n_1 and n_2 denoting the number of positive and negative values in the series.

The runs test rejects the null hypothesis if

$$|Z| > Z_{1-\alpha/2}$$

For a large-sample runs test (where $n_1 > 10$ and $n_2 > 10$), the test statistic is compared to a standard normal table. That is, at the 5 % significance level, a test

statistic with an absolute value greater than 1.96 indicates non-randomness. For a small-sample runs test, there are tables to determine critical values that depend on values of n_1 and n_2.

3.3.3 Generalized extreme values distribution

The GEV distribution function combines three asymptotic forms of extreme value distributions, Gumbel, Weibull and Frechet (Fisher and Tippett 1928), in a unique form, defined according to Jenkinson (1955) as follows:

$$F(x) = \exp[-\left(1-\xi\frac{x-\mu}{\sigma}\right)^{\left(\frac{1}{\xi}\right)}, if\ \xi \neq 0$$

$$F(x) = \exp\left[-exp\left(-\frac{x-\mu}{\sigma}\right)\right] if\ \xi = 0$$

Where,

μ is the location parameter $-\infty < \mu < \infty$;

σ is a scale parameter $0 < \sigma < \infty$; and

ξ is the shape parameter with $-\infty < \xi < \infty$.

The extreme value distribution of Weibull and Fréchet corresponds to the particular cases where $\xi < 0$ and $\xi > 0$, respectively. When $\xi = 0$, the function assumes a form which represents a Gumbel distribution. For the quantile xP of GEV distribution, with the return period T, the cumulated probability is given by F(xP)=1-(1/T), which results in (Palutikof *et al.*, 1999):

$$x_p = \mu + \frac{\sigma}{\xi}\left[1-\left(-ln\left(1-\frac{1}{T}\right)\right)^{\xi}\right], if\ \xi \neq 0$$

$$x_p = \mu - \sigma ln\left[-ln\left(1-\frac{1}{T}\right)\right] if\ \xi = 0$$

In GEV distribution, the sample is divided in sub-periods (blocks) that may be monthly, seasonal or annual, etc. From each block, a maximum or minimum value is extracted, to compose a set of extreme data, according to the block

maximum methodology, or annual maximums (Maraun *et al.*, 2009; Sugahara *et al.*, 2009). In this study, in the GEV distribution, the annual maximums were considered as extremes, through the block maxima method. As the study period is from 1951 to 2008 (30 years), the final dataset consists in 58 observations of annual maximums of precipitation.

3.3.4 Q-Q plot

To verify the quality of the parameters from the EVT distributions, the quantile–quantile (Q-Q) plot will be analysed, since it is one of the most used methods in the verification for fitting the theoretical distribution to the empirical one, consisting in the graphical comparison of theoretical quantiles of the distribution, with the quantiles of sample data, showing the relationship between the fitted and the observed data.

The quantile-quantile (q-q) plot is a graphical technique for determining if two data sets come from populations with a common distribution.

A q-q plot is a plot of the quantiles of the first data set against the quantiles of the second data set. A quantile refers to a fraction (or percent) of points below the given value. That is, the 0.3 (or 30%) quantile is the point at which 30 percent of the data fall below and 70 percent fall above that value.

A 45-degree reference line is also plotted. If the two sets come from a population with the same distribution, the points should fall approximately along this reference line. The greater the departure from this reference line, the greater the evidence for the conclusion that the two data sets have come from populations with different distributions.

In the current study, q-q plots have been plotted using Easyfit software.

3.3.5 Kolmogorov Smirnov test

Graphical methods such as q-q plot are subject to mistakes, once they depend on the visual interpretation. For a more objective result, a non-parametric test was used—the Kolmogorov–Smirnov (KS) test (Chakravarti et al. 1967).

The Kolmogorov-Smirnov (K-S) test is based on the empirical distribution function (ECDF). Given *N ordered* data points Y_1, Y_2, ..., Y_N, the ECDF is defined as

$$E_N = n(i)/N$$

where *n(i)* is the number of points less than Y_i and the Y_i are ordered from smallest to largest value. This is a step function that increases by $1/N$ at the value of each ordered data point. An attractive feature of this test is that the distribution of the K-S test statistic itself does not depend on the underlying cumulative distribution function being tested.

In the KS test, the following null hypothesis is considered

H0: F(x)= G(x) The data follows a specified distribution

and the alternative hypothesis is

H1: F(x)≠G(x). The data do not follow a specific distribution.

The test statistic is obtained by

$$D = \max_{1 \le i \le N} -\frac{i-1}{N}, \frac{i}{N} - F(Y_i))$$

Where,

F(x) is the theoretical cumulative distribution function and

G(x) is the empirical cumulative distribution function, to n random observations with a cumulative distribution function.

This test represents the upper extreme limit of differences between absolute values of the empirical and theoretical cumulative distribution considered in the test (Lucio, 2004). The null hypothesis is rejected if the D value is greater than the

tabulated one. This is equivalent to consider that the exact probability of the test is lower than the significance level. Hence, the KS test was applied to compare the goodness of fit of the GEV distribution, with a significance level of 5 per cent. The K-S test in this study was carried out using Easyfit Software.

CHAPTER 4

RESULTS AND DISCUSSION

The study area of Western Ghats and its 32 constituent grids are analysed for trends in summer monsoonal rainfall extremes and the results are presented and discussed in this section.

4.1 RAINFALL ANALYSIS

The mean annual monsoonal rainfall over the study area is 1616.15 mm and the standard deviation is 242.966. Table 2 shows the mean annual summer monsoonal rainfall for the constituent grids.

It was observed that the mean annual monsoonal rainfall varies from 231.4 mm in grid 117 to 3416 mm in grid 253.

On running the Mann-Kendall test on annual mean rainfall data in 5 per cent significance, the results in Table 3 as shown in were obtained. If the p value is less than the significance level α (alpha) = 0.05, H_0 (null hypothesis) is rejected. Rejecting H_0 indicates that there is a trend in the time series, while accepting H_0 indicates no trend was detected. On rejecting the null hypothesis, the result is said to be statistically significant. The annual monsoonal rainfall for the whole region is plotted below with its trend line in Figure 3.

However, no significant trend has been found when analysed with Mann Kendall method of trend analysis. Thus, mean annual rainfall as a sole parameter for climate change analysis falls short. This may be due to the fact that averages do not often give the whole picture as it compensates for the varying trends over the years by nullifying the effects of trends of constituent events to the mean rainfall like moderate and high intensity rainfall events.

Table 2. Mean Annual Rainfall over constituent grids.

Grid Index	Average Rainfall (mm)	Grid Index	Average Rainfall (mm)
81	875.1	289	1480.9
115	1812.0	323	1976.7
116	933.1	324	764.0
117	231.4	357	3239.2
150	1923.7	358	1855.6
151	894.8	359	437.6
152	287.2	392	2922.3
184	3029.6	393	1857.8
185	1964.0	394	493.6
186	641.9	427	2501.3
219	3017.3	428	1633.0
220	1486.9	429	521.4
253	3416.0	462	2121.7
254	2300.2	463	1360.1
255	726.1	497	1433.1
288	2541.1	498	1057.4

Table 3. Parameters of Mann Kendall Trend analysis for mean annual monsoonal rainfall

Kendall's tau	-0.056
S	-93.000
Var(S)	22223.667
p-value (Two-tailed)	0.537
Alpha	0.050

4.2 ONE DAY MAXIMUM RAINFALL

The one day maximum rainfall extracted from the 32 constituent grids for the entire period showed a variation from 118.63 mm in 1981 to 316.63 mm in 2005. The one day maximum values for the region is given in table 4.

The temporal variation in one day maximum rainfall for the time series is shown in figure 4. along with its trend line. A significant trend is observed in the series. The values are seen to be increasing steadily and a profound increase is observed in the recent decades after 1980. The strength of the test statistic confirms that the number of events of 1-day maximum rainfall over the basin has increased considerably. The parameters of the trend analysis are given in Table 4.

A recent study in the Narmada basin involving 23 grids (Thomas et.al., 2015), carried out a similar trend analysis on the one day maximum rainfall series for the time period of 1951-2008. The 1-day maximum rainfall extracted from the 23 grids covering the Narmada basin for the entire period exhibited a variation from 135.4 to 473.0 mm and a positive trend at 95 per cent significance level with the MK test value of 3.66 indicating a considerable increase in the one day maximum rainfall events. The climate in Narmada basin which is located in Central India unlike the current study area has the seasonal mean climate and the daily variability reasonably homogeneous (Goswami *et.al.*, 2006). One day maximum rainfall exhibiting a rising trend in a more variable climate of the Ghats thus indicate that analogous trends exist in larger parts of the Indian Subcontinent.

Based on these results, it becomes imperative to think on the ecological, economic, and social impacts that could result if increasing precipitation trends continue in the region in the future. For coastal areas, in particular tropical storms, and coastal storms form a major hazard. The vulnerability to storms might further be aggravated if extreme rainfall episodes continue in the future and consequently result in inland and coastal flooding. Institutional changes, coastal regulation, and management goals have to be, therefore, adapted in a timely manner.

Table 4. One Day Maximum Rainfall Values for ISMR over the Western Ghats

Year	ODMR (mm)	Year	ODMR mm)	Year	ODMR (mm)
1951	172.20	1971	204.03	1990	180.66
1952	161.59	1972	146.29	1991	246.69
1953	180.18	1973	148.55	1992	181.84
1954	251.98	1974	180.38	1993	179.76
1955	152.40	1975	175.71	1994	172.68
1956	148.19	1976	230.73	1995	194.20
1957	157.16	1977	158.63	1996	223.04
1958	218.89	1978	171.97	1997	203.84
1959	162.08	1979	160.67	1998	194.35
1960	181.31	1980	177.35	1999	290.57
1961	210.02	1981	118.63	2000	173.34
1962	181.60	1982	219.10	2001	124.79
1963	178.26	1983	204.54	2002	271.34
1964	171.28	1984	227.95	2003	271.68
1965	233.35	1985	148.79	2004	216.71
1966	202.00	1986	176.95	2005	316.63
1967	183.54	1987	141.97	2006	216.59
1968	207.15	1988	149.52	2007	262.69
1969	146.35	1989	232.82	2008	173.22
1970	177.91				

Table 5. Parameters of Mann Kendall trend analysis for One Day Maximum Rainfall over the period 1951-2008

Kendall's tau	0.204
S	337.000
Var(S)	22223.667
p-value (Two-tailed)	0.024
alpha	0.050

The time series of the 1-day maximum rainfall has further been analysed to identify the variation in the initial 20-year period (1951–1970) and the recent 20-year period (1989–2008), and the results are given in Table 5. This was to observe the contrast in the One Day Maximum Rainfall in the recent decades of warming when compared to the earlier times.

It was observed that the average of the values has shifted from 183.37 mm in the initial period to 216.37 mm (Table 6.) in the latter period. There has been a significant increase in maximum of the one day maximum rainfall from the former to latter period. This indicates that the magnitude of rainfall has considerably increased in the later parts of the last 58 years. The minimum of the one day maximum rainfall has decreased from 143.35 in 1951-1970 to 124.79 in the recent period which occurred in 2001. Also, there were only 6 events of rainfall greater than 200 mm in the former period whereas 11 events occurred in the latter period. For events, greater than 300 mm, there was no such occurrence in the former period and a single event has been recorded in the period of 1989-2008. These shifts could not be the products of climate variability and are in concurrence with the significant rising trends in One Day Maximum Rainfall over the region in the backdrop of a changing environment. The analysis of the above parameters at Narmada basin (Thomas *et.al.*, 2015) too had a comparable result. One day maximum rainfall was seen to have increased significantly from 203.9 mm during 1951–1970 to 275.9 mm during the latter 20-year period. A positive upward shift was also observed in the minimum (and maximum as well) of the 1-day maximum rainfall series when compared between the first two decades. The major contrast between the two studies is that the minimum of the one day maximum rainfalls did not show an increase in this study as seen in the Narmada basin case.

4.2.1 One day maximum rainfall values in the latitudes

In the current scope of the study, the Western Ghats region has its constituent grids falling in 13 latitudes starting from 9°N in the southern peninsula to 21°N in the upper parts of the Ghats. The grids contained in each latitude is given in Table 7.

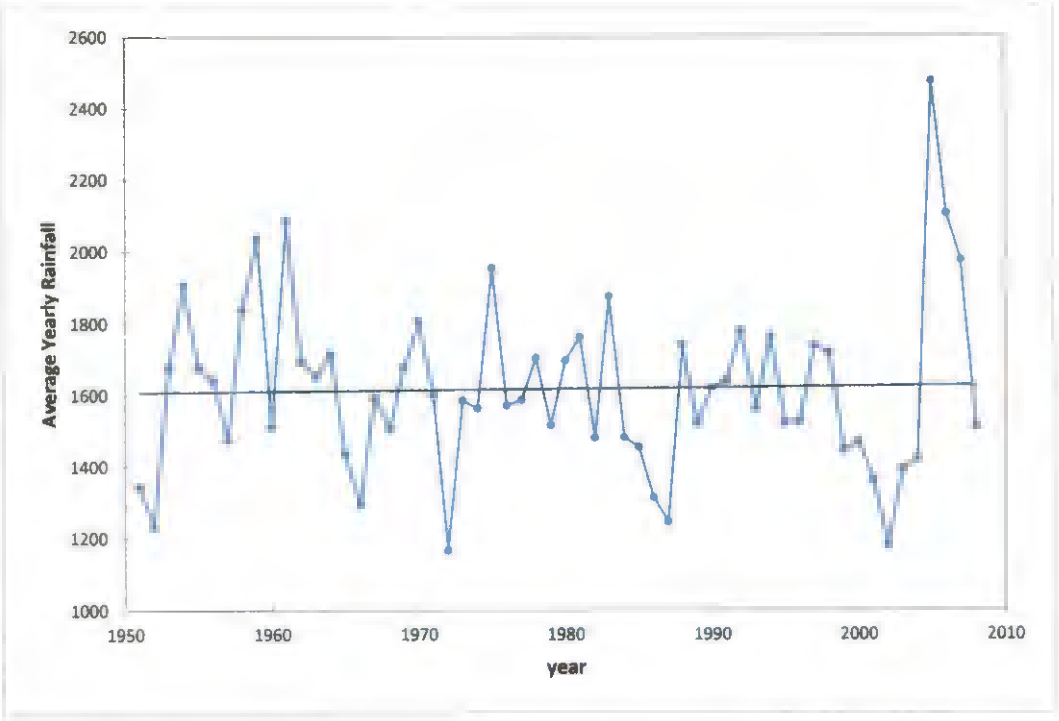

Figure 3. Temporal Analysis of Mean Annual Rainfall over Western Ghats

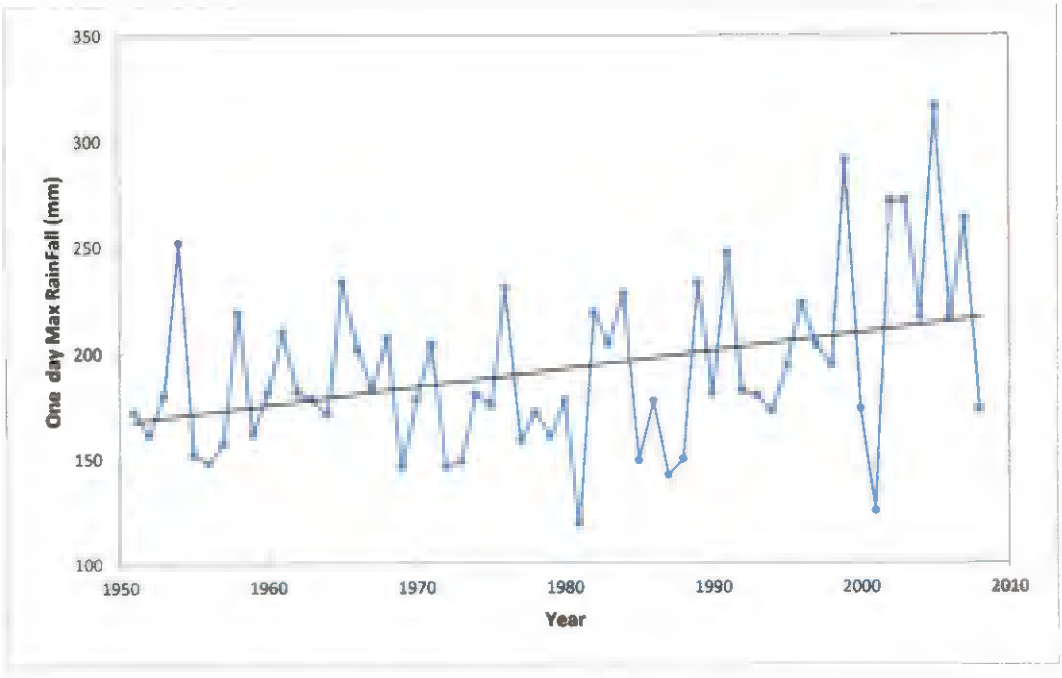

Figure 4. Temporal Analysis of ODMR over Western Ghats

Table 6. Statistical Parameters associated with One Day Maximum Rainfall over the split periods of 1951-1970 and 1989-2008

Statistical Parameters	1951-1970	1989-2008
Average of One Day Maximum Rainfall (mm)	183.87	216.37
Maximum of One Day Maximum Rainfall (mm)	251.98	316.63
Minimum of One Day Maximum Rainfall (mm)	143.35	124.79
Number of events with rainfall >200 mm	6	11
Number of events with rainfall >300 mm	0	1

Table 7. Grids of Respective Latitudes

Latitude	Grid Index
9 N	81
10 N	115, 116. 117
11 N	150, 151, 152
12 N	184, 185, 186
13 N	219, 220
14 N	253, 254, 255
15 N	288, 289
16 N	323, 324
17 N	357, 358, 359
18 N	392, 393, 394
19 N	427, 428, 429
20 N	462, 463
21 N	497, 498

By combining the data of the constituent grids in each latitude and extracting the annual maximums, the one day maximum rainfall for respective latitudes are tabulated in Table 8. Mann Kendall Trend analysis was carried out on each latitude and the temporal variation in the time series are plotted which are represented in figure 5. The trend analysis parameters are tabulated in Table 8.

The test Interpretation in the tabulation is shown to have inputs of either 'Accept H0' or 'Reject H0'. 'Accept H0' refers to accepting the null hypothesis of having no trend in the trend test and 'Reject H0' refers to rejecting the notion of having no trend and thus implying that a significant trend is present. The P-value in the test needs to be less than the alpha value which is taken as 0.05 by default in the test to obtain a trend.

Two latitudes are seen to have significant positive trends in One Day Maximum Rainfall in the whole region. The latitudes are 14°N and 21°N. They have P value of 0.049 and 0.012 (null hypotheses of having no trend was rejected) respectively which are less than 0.05. There are other latitudes which have very low P values showing a positive trend but not low enough to exhibit a significant trend. Figure 5a. and Figure 5b. shows the temporal distribution in ODMR for the latitudes of 14°N and 21°N.

Table 8. Parameters of Mann Kendall trend analysis for One Day Maximum Rainfall over the constituent latitudes of Western Ghats for the period 1951-2008

Latitude	Kendall's Tau	Mann Kendall Statistic	Var (s)	P-value (two tailed test)	alpha	Test Interpretation
9 N	-0.151	-249.000	22223.667	0.096	0.05	Accept H0
10 N	0.025	41.000	22223.667	0.788	0.05	Accept H0
11 N	-0.024	-39.000	22223.667	0.799	0.05	Accept H0
12 N	0.020	33.000	22223.667	0.830	0.05	Accept H0
13 N	0.057	95.000	22223.667	0.528	0.05	Accept H0
14 N	0.177	293.000	22223.667	0.049	0.05	Reject H0
15 N	0.153	253.000	22223.667	0.091	0.05	Accept H0
16 N	0.126	209.000	22223.667	0.163	0.05	Accept H0
17 N	-0.107	-177.000	22223.667	0.238	0.05	Accept H0
18 N	0.056	93.000	22223.667	0.537	0.05	Accept H0
19 N	0.149	247.000	22223.667	0.099	0.05	Accept H0
20 N	0.140	231.000	22223.667	0.123	0.05	Accept H0
21 N	0.228	377.000	22223.667	0.012	0.05	Reject H0

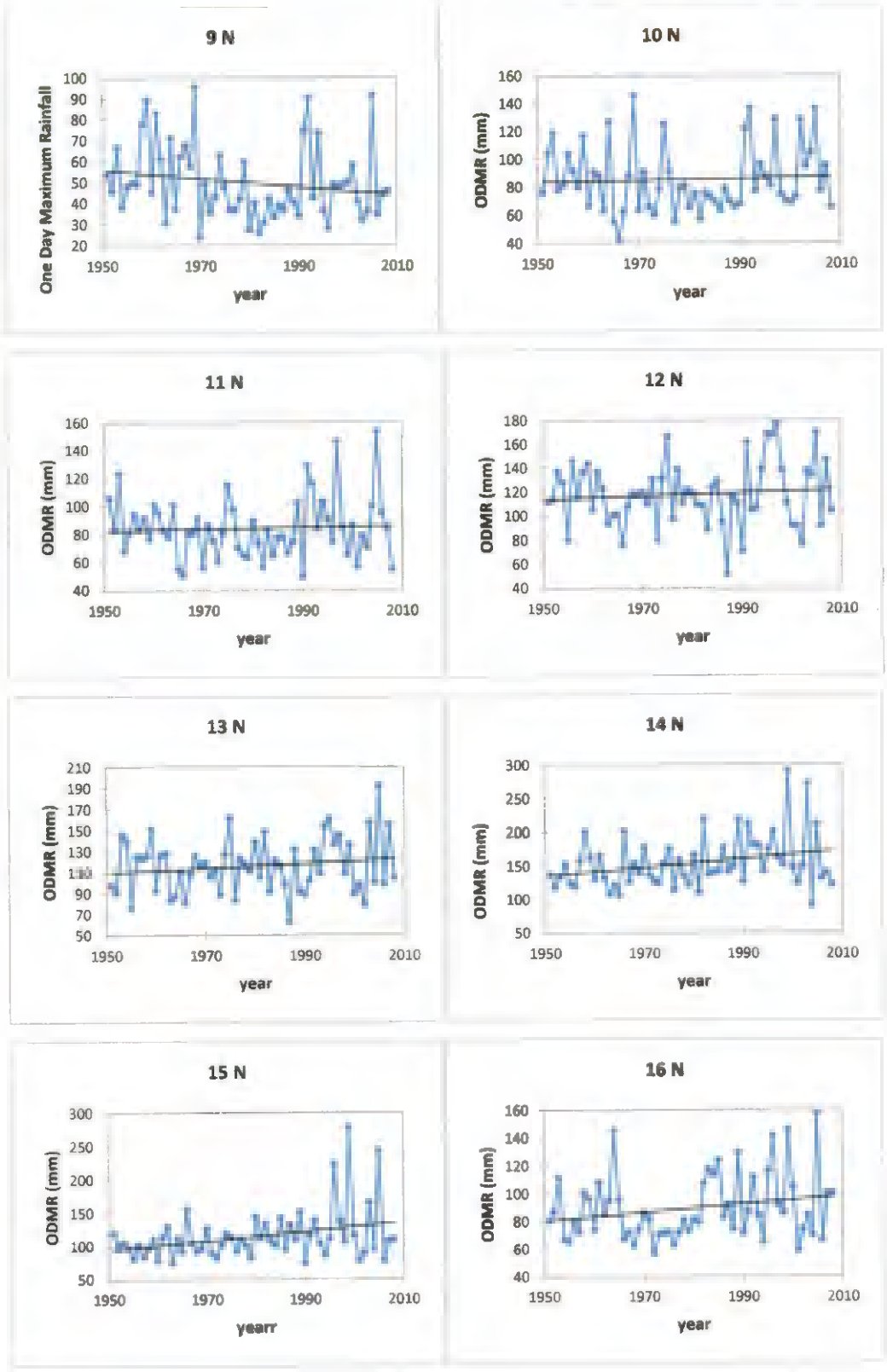

Figure 5a. Temporal Analysis of ODMR over constituent latitudes (9°N-16° N)

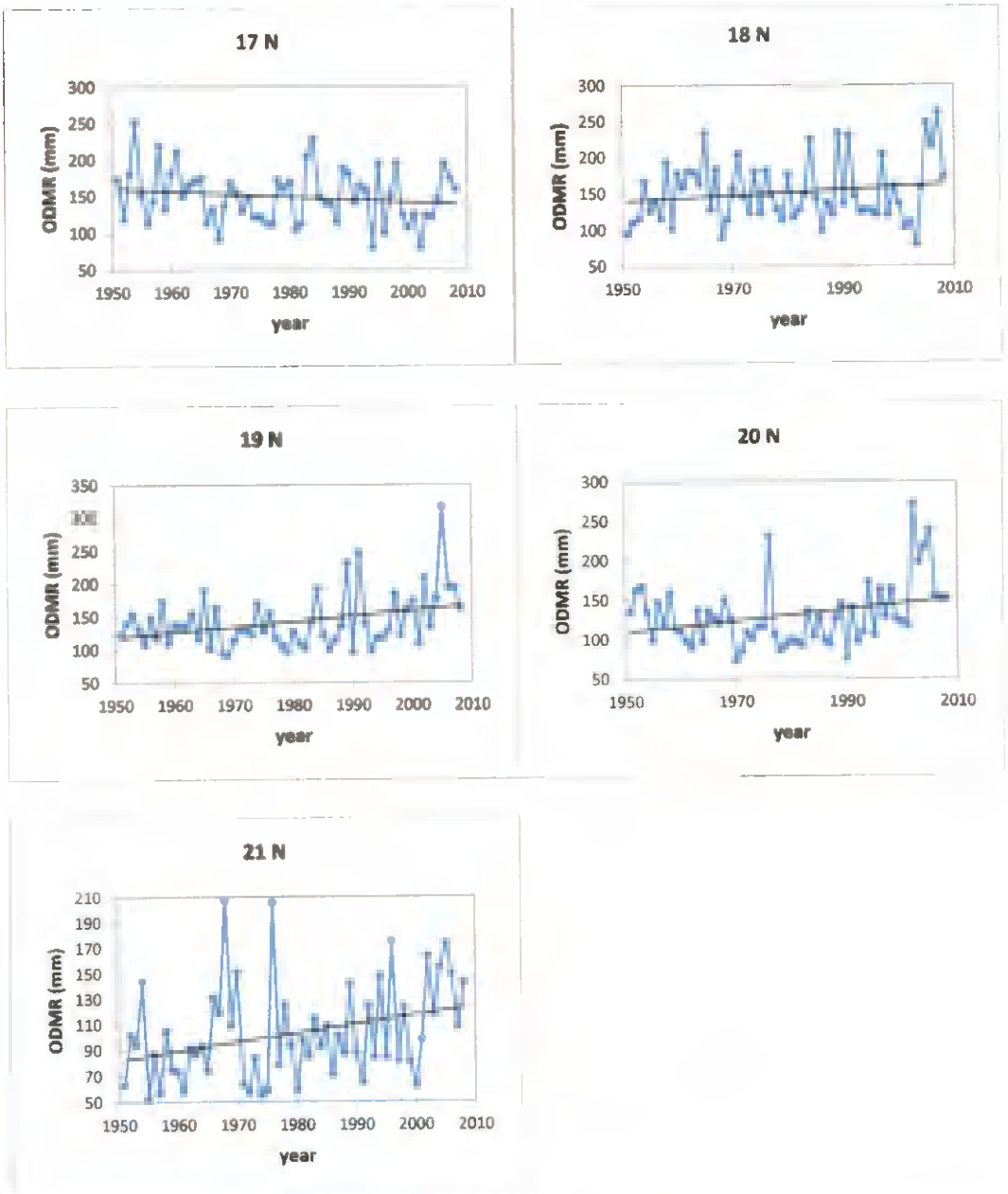

Figure 5b. Temporal Analysis of ODMR over constituent latitudes (17°N-21° N)

4.2.2 One Day Maximum Rainfall Trends in Grids

There are 32 (1° x 1° resolution) grids in the study area. Temporal analysis of the annual maximum rainfall is done using Mann Kendall method and trends are analysed. The time series graphs of the grids are plotted on Figure 6. The parameters of trend analysis are given in Table 9. The MK statistic, P value, alpha value, Variance, Test statistic, Correlation factor (tau) and test interpretation are given. The test interpretation as in the earlier cases is either 'Accept H0' referring to no significant trend or 'Reject H0' implicating a significant trend.

It is observed from the tabulation that there are 7 grids out of the 32 grids which show a significant rising trend in one day maximum rainfall. The grids are 186, 359, 394, 428, 429, 497 and 498.

Table 9. Parameters of Mann Kendall trend analysis for One Day Maximum Rainfall over the constituent grids of Western Ghats for the period 1951-2008

Grid	Kendall's Tau	Mann Kendall Statistic	Var (s)	P-value	alpha	Test Interpretation
115	0.013	21.000	22223.667	0.893	0.05	Accept H0
116	-0.033	-55.000	22223.667	0.717	0.05	Accept H0
117	0.082	135.000	22223.667	0.369	0.05	Accept H0
150	-0.031	-51.000	22223.667	0.737	0.05	Accept H0
151	-0.153	-253.000	22223.667	0.091	0.05	Accept H0
152	0.114	189.000	22223.667	0.207	0.05	Accept H0
184	0.028	47.000	22223.667	0.758	0.05	Accept H0
185	-0.022	-37.000	22223.667	0.809	0.05	Accept H0
186	-0.195	-323.000	22223.667	0.031	0.05	Reject H0
219	0.057	95.000	22223.667	0.528	0.05	Accept H0
220	0.027	45.000	22223.667	0.768	0.05	Accept H0
253	0.177	293.000	22223.667	0.050	0.05	Accept H0
254	0.146	241.000	22223.667	0.107	0.05	Accept H0
255	-0.003	-5.000	22223.667	0.979	0.05	Accept H0
288	0.153	253.000	22223.667	0.091	0.05	Accept H0
289	-0.004	-7.000	22223.667	0.968	0.05	Accept H0
323	0.126	209.000	22223.667	0.163	0.05	Accept H0
324	0.126	209.000	22223.667	0.163	0.05	Accept H0
357	-0.107	-177.000	22223.667	0.238	0.05	Accept H0
358	-0.022	-37.000	22223.667	0.809	0.05	Accept H0
359	0.194	321.000	22223.667	0.032	0.05	Reject H0
392	0.051	85.000	22223.667	0.573	0.05	Accept H0
393	0.021	35.000	22223.667	0.820	0.05	Accept H0
394	0.229	379.000	22223.667	0.011	0.05	Reject H0
427	0.135	223.000	22223.667	0.136	0.05	Accept H0
428	0.263	435.000	22223.667	0.004	0.05	Reject H0
429	0.224	371.000	22223.667	0.013	0.05	Reject H0
462	0.131	217.000	22223.667	0.147	0.05	Accept H0
463	0.112	185.000	22223.667	0.217	0.05	Accept H0
497	0.243	401.000	22223.667	0.007	0.05	Reject H0
498	0.226	373.000	22223.667	0.013	0.05	Reject H0
81	-0.151	-249.000	22223.667	0.096	0.05	Accept H0

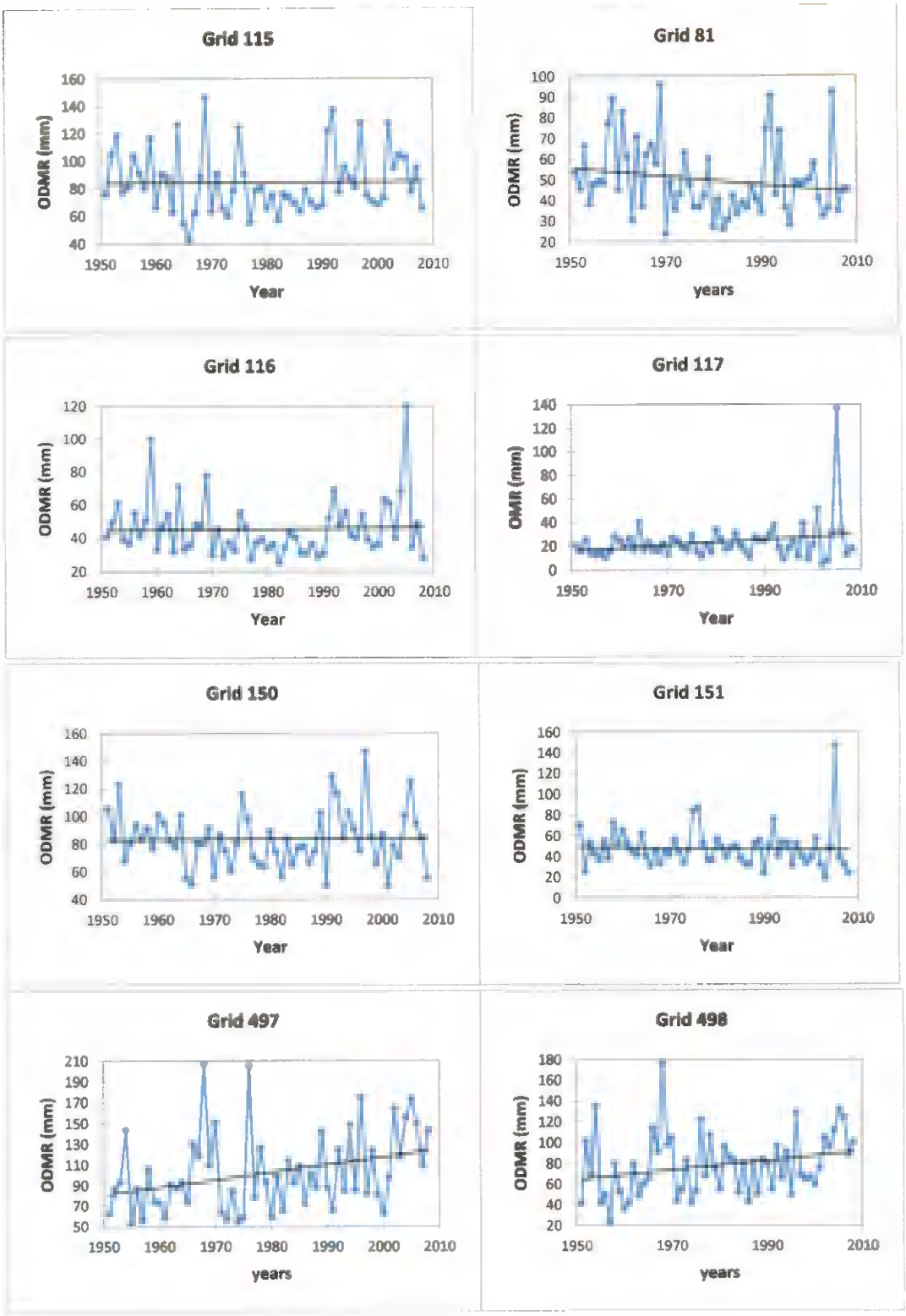

Figure 6a. Temporal analysis of ODMR over the constituent grids (81, 115, 116, 117, 150, 151, 497 and 498)

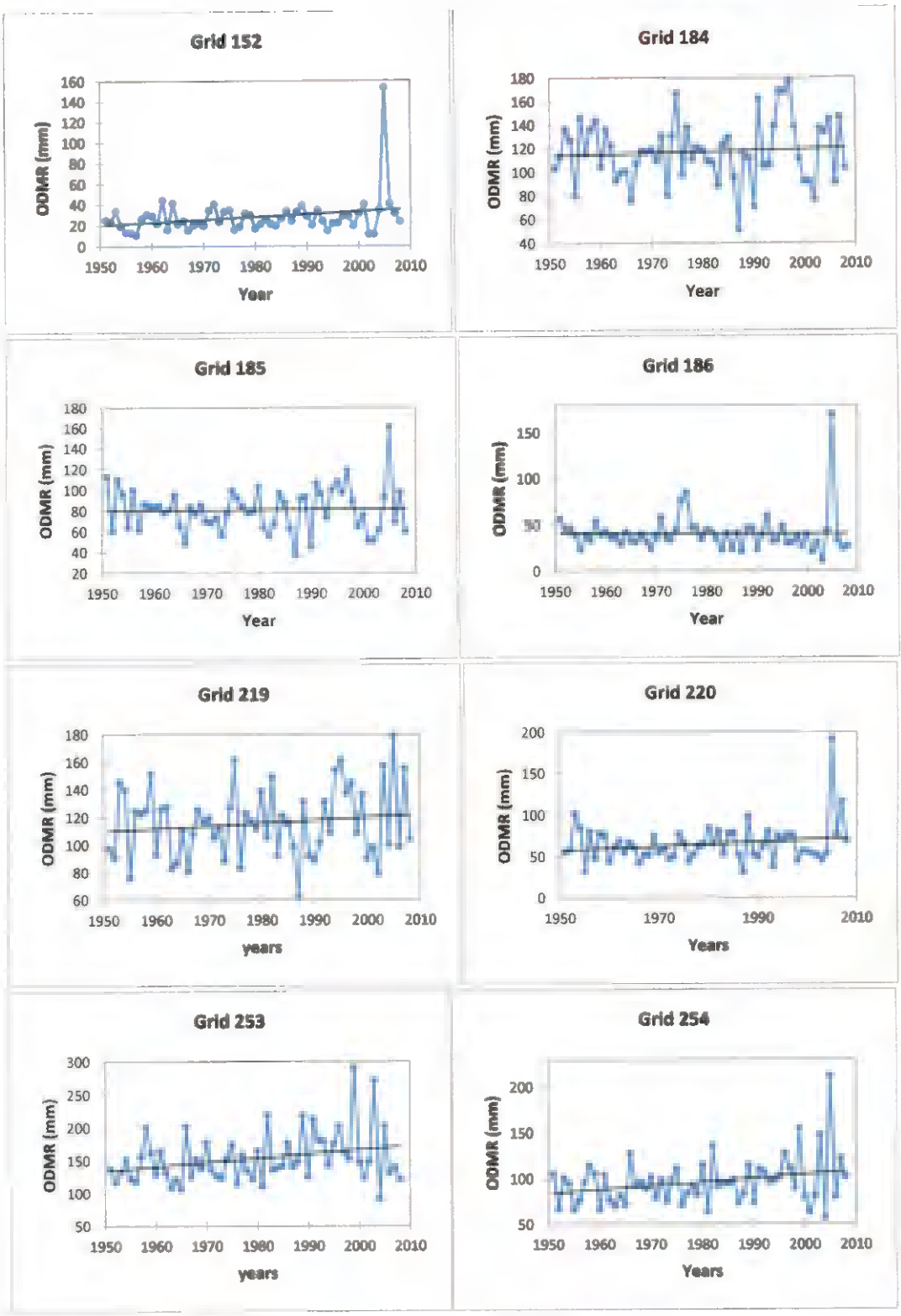

Figure 6b. Temporal analysis of ODMR over the constituent grids (152, 184, 185, 186, 119, 220, 253 and 254) in Western Ghats

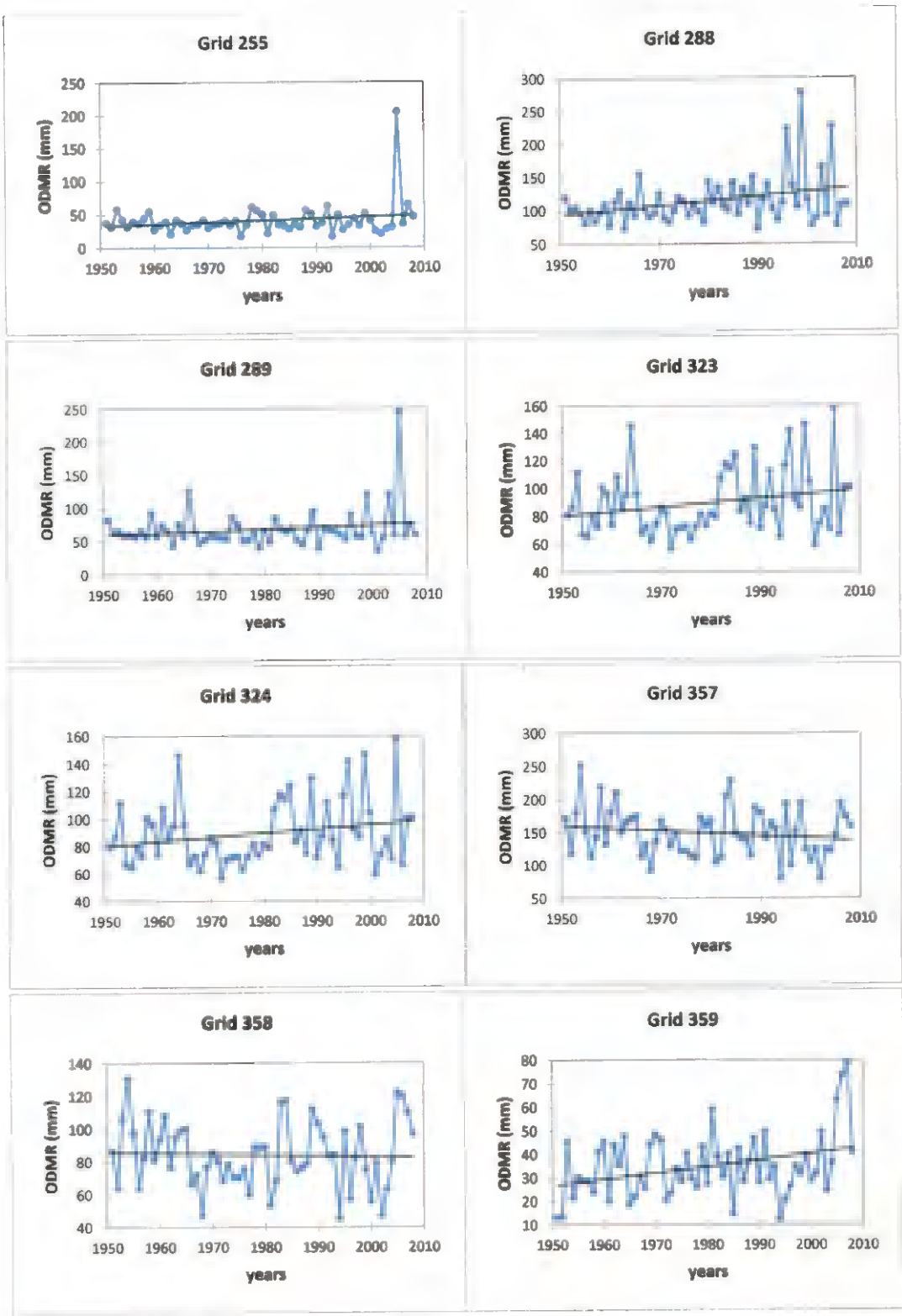

Figure 6c. Temporal analysis of ODMR over the constituent grids (255, 288, 289, 323, 324, 357, 358 and 359) in Western Ghats

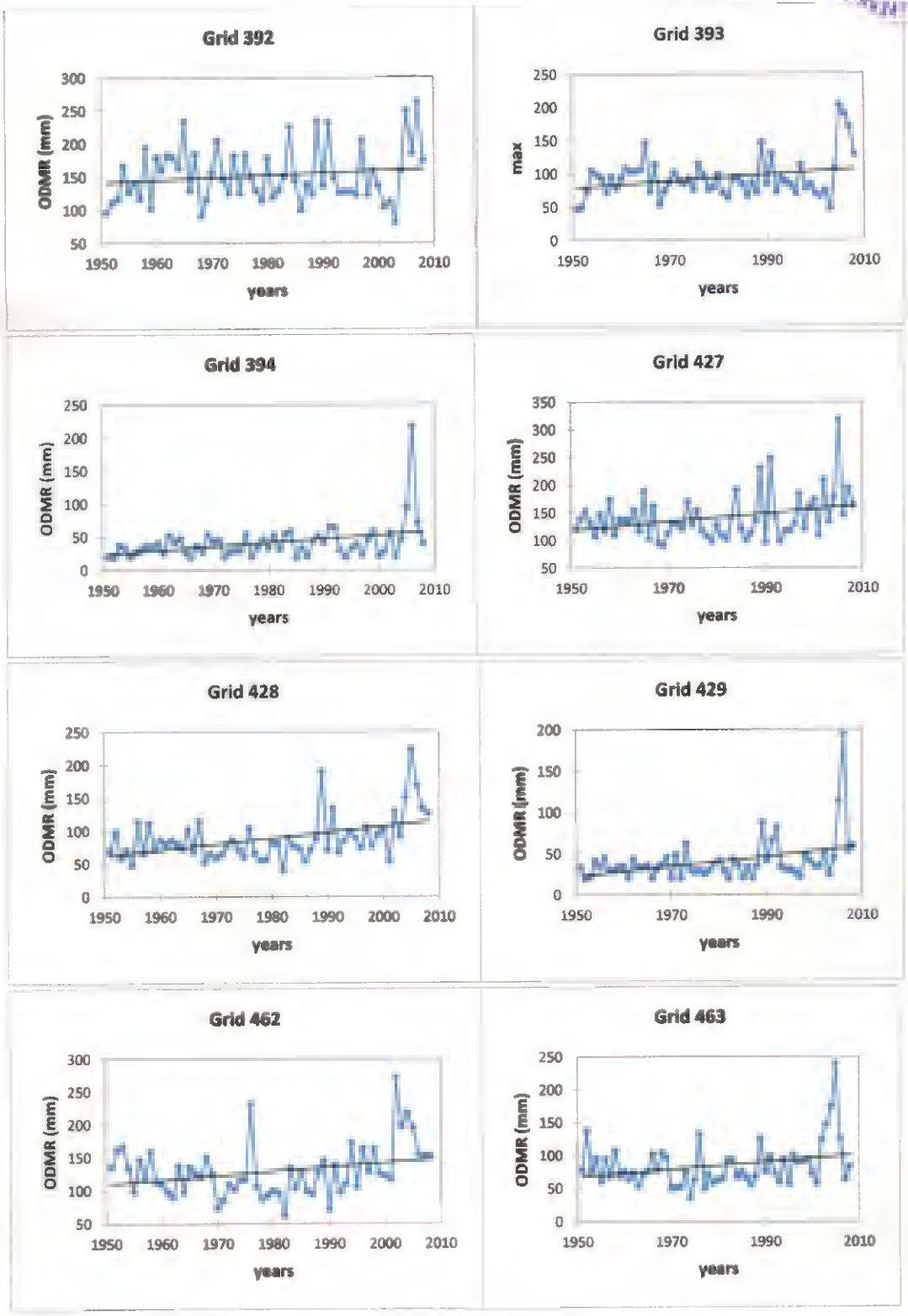

Figure 6d. Temporal analysis of ODMR over the constituent grids (392, 393, 394, 427, 428, 429, 462 and 463) in Western Ghats

4.2.3 Shift of dates of one day maximum rainfall

The shift in dates of the occurrence of the annual maximum rainfall for the study area is found out and plotted as a histogram. The chronological day of occurrence of the annual maximum rainfall of the summer monsoonal season for the whole Western Ghats region is tabulated (Table 10.) and plotted. The significance of the shift was also calculated (Figure 7.).

It has been observed from the table that during the recent few years, the occurrence of One day maximum Rainfall has shifted to the far end of the season as in years 2006 and 2008 respectively when the ODMR occurred on the 98th and 72nd day respectively. The trends in shift analysis showed that the time series was not significant. This shift in dates could be attributed to the inherent variability of the noisy monsoonal system.

4.3 CHANGE IN FREQUENCY OF HIGH INTENSITY RAINFALL

Frequency analysis of the 3 types of high Intensity rainfalls are carried out.

1. Heavy Rainfall Events. (>100 mm and <150 mm)
2. Very Heavy Rainfall Events. (>150mm and <200 mm)
3. Extreme Events. (>200 mm)

4.3.1 Temporal distribution of high intensity rainfall

The number of grids getting the above three types of rainfall are analysed over the entire study period.

4.3.1.1 Heavy rainfall events

The Temporal analysis of grids having heavy rainfall events over the period 1951-2008 is given on Figure 8. The Mann Kendall analysis parameters are given on Table 11. A significant rising trend is observed in the number of grids experiencing heavy rainfall events.

4.3.1.2 Very heavy rainfall events

Temporal analysis of very heavy rainfall events for the period 1951-2008 yielded a significant rise in their occurrences. More number of grids experienced heavy rainfall events as evident from the graphical representation (Figure 9.). The Mann Kendall trend analysis parameters are given on Table 11.

4.3.1.3 Extreme rainfall events

Similarly, to the earlier two rainfall events, extreme rainfall was also analysed for temporal distribution in grids. The graphical representation is given on Figure 10. The statistical parameters of Mann Kendall analysis are given on Table 11.

A rising trend in extreme rainfall events was observed over the study area for the period 1951-2008.

Table 10. Chronological day of occurrence for One day maximum rainfall for the Western Ghats region for the period 1951-2008

Year	Day of occurrence	Year	Day of Occurrence	Year	Day of Occurrence
1951	12	1971	24	1990	78
1952	55	1972	32	1991	10
1953	31	1973	35	1992	29
1954	64	1974	35	1993	55
1955	29	1975	22	1994	43
1956	63	1976	61	1995	62
1957	39	1977	49	1996	15
1958	26	1978	16	1997	84
1959	48	1979	26	1998	30
1960	55	1980	32	1999	12
1961	26	1981	54	2000	43
1962	38	1982	64	2001	65
1963	37	1983	29	2002	27
1964	68	1984	31	2003	22
1965	46	1985	62	2004	64
1966	60	1986	16	2005	57
1967	58	1987	31	2006	98
1968	67	1988	13	2007	24
1969	54	1989	54	2008	72
1970	49				

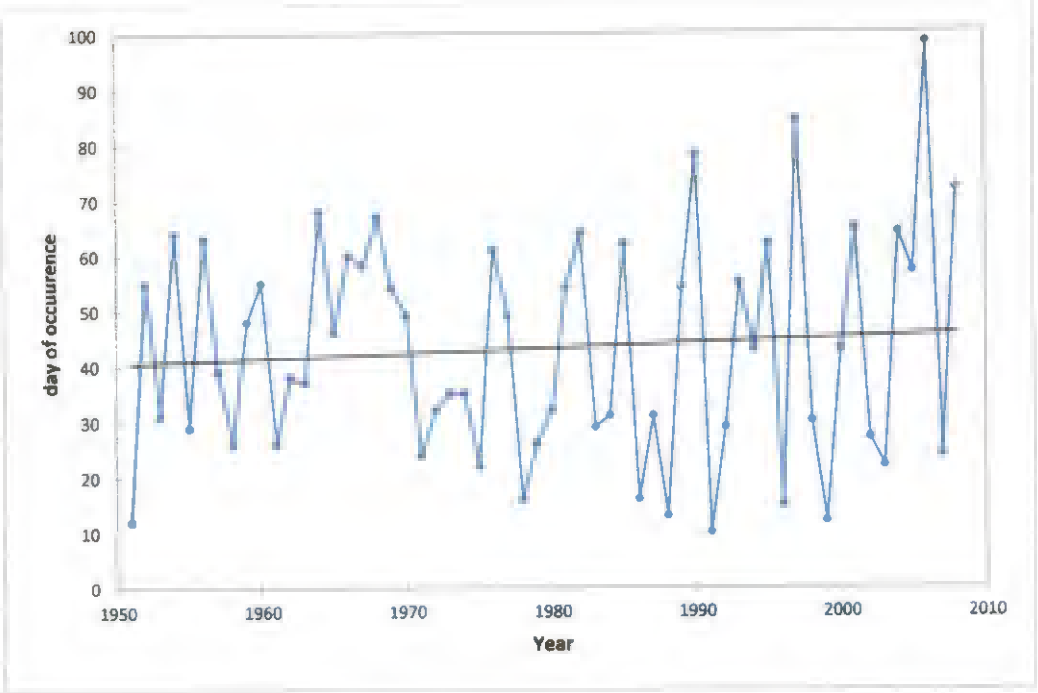

Figure 7. Significance in shift of days

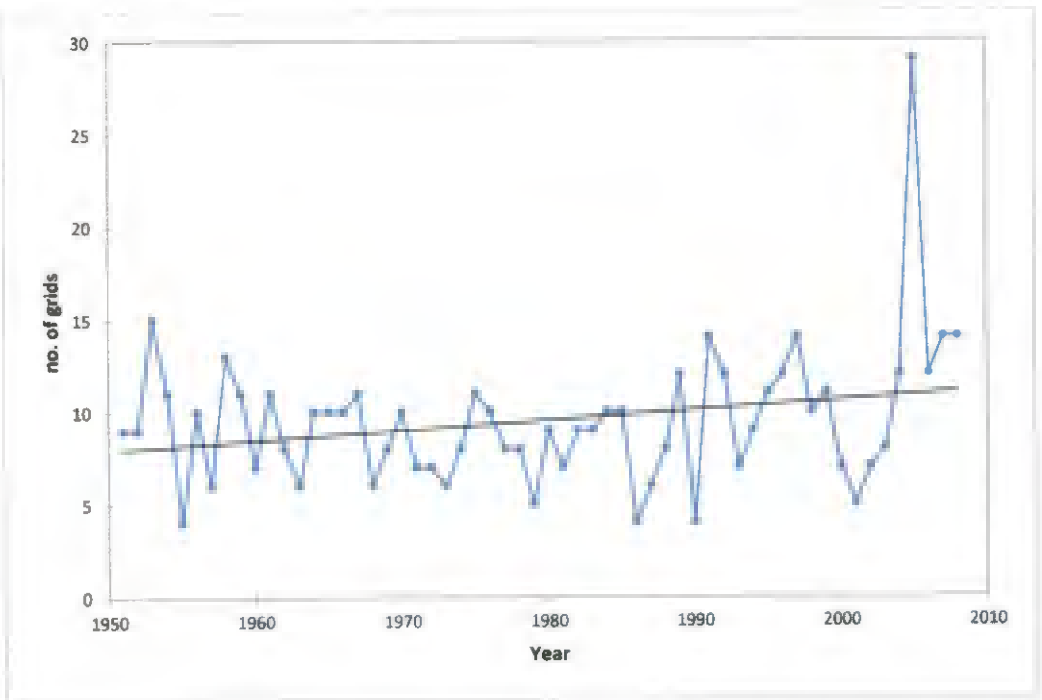

Figure 8. Temporal analysis of grids getting heavy rainfall events

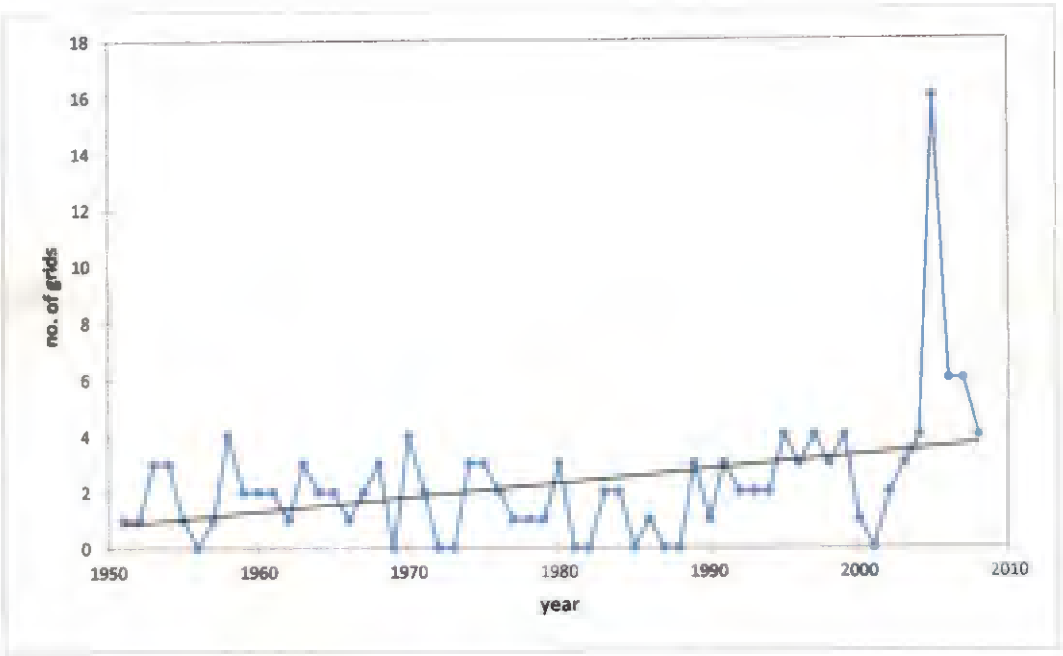

Figure 9. Temporal analysis of grids getting very heavy rainfall events

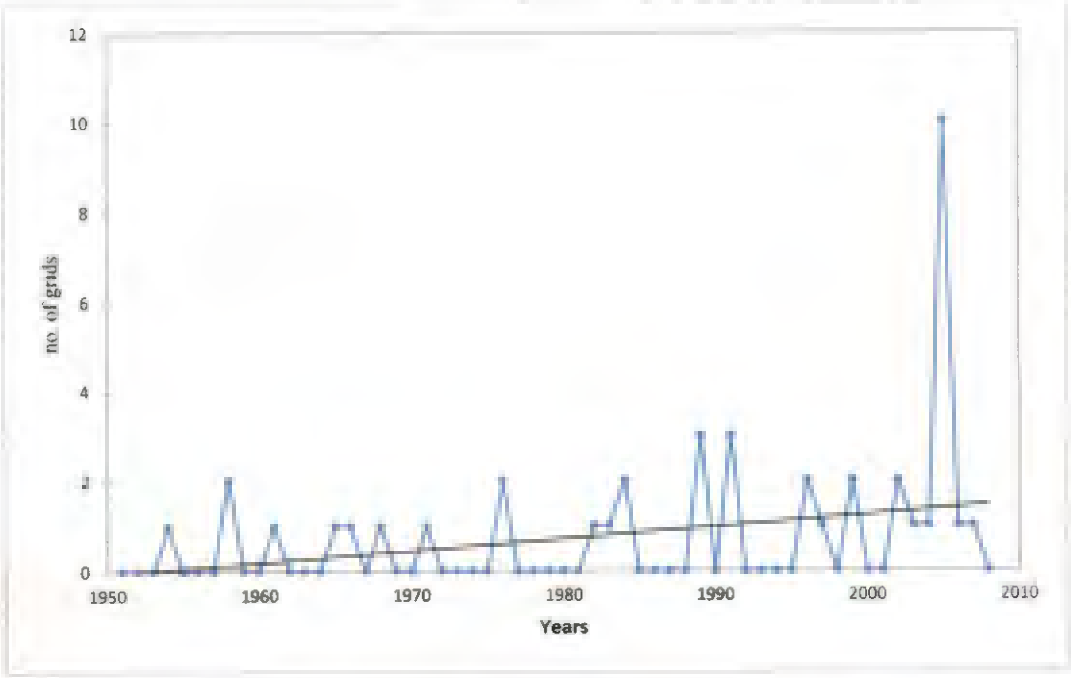

Figure 10. Temporal analysis of grids getting extreme rainfall events

4.3.2 Occurrence Frequency of High Intensity Rainfalls

The number of instances of occurrence of high intensity rainfall events in the total study area in each year is done for the entire period of 1951-2008 and also for the split periods of 1951-1970 and 1989-2008. Frequency analysis is done for checking trends. The frequency analysis of moderate events is also done for a comparison.

4.3.2.1 Heavy rainfall events

The Heavy Rainfall events did not show a significant trend even though a rising trend of its occurrence is found. The graph of its annual frequency is given in Figure 11. The Mann Kendall Parameters are given in Table 12.

4.3.2.2 Very heavy rainfall events

There has been a steady increase in the yearly frequency of very heavy rainfall events. The trend is significant as represented in Figure 12. The statistical Parameters of the trend analysis are given in Table 12.

4.3.2.3 Extreme Events

Extreme events (>200mm) have exhibited an evident increase in its occurrence. The trend analysis is done as represented in Figure 13. The statistical parameters of the Mann Kendall trend analysis are given in table.

4.3.2.4 Moderate Rainfall Events

Moderate events are those which come in between 2.5 and 100 mm of rainfall intensity and they form the major share of rainfall events that occur here. The graphical representation of yearly frequency of moderate events is given in Figure 14. The statistical parameters of Mann Kendall trend analysis are given in Table 12.

Even though a decreasing trend in moderate rainfall events are seen, they are not significant. The decrease in moderate events may have occurred at the expense of increase in very heavy rainfall events.

Table 11. Statistical Parameters of Mann Kendall Trend analysis for Temporal Distribution of high intensity rainfall events of heavy, very heavy and extreme magnitudes on grids

	No. of Heavy Rainfall Events	No. of Very Heavy Rainfall Events	No of Extreme Rainfall Events
Kendall's tau	0.130	0.235	0.212
S	205.000	353.000	263.000
Var(S)	21923.667	21294.333	16535.667
p-value (Two-tailed)	0.168	0.016	0.042
alpha	0.050	0.050	0.050

Table 12. Statistical Parameters of Mann Kendall Trend Analysis for frequency analysis of high intensity and moderate rainfall events

	Heavy Rainfall Events	Very Heavy Rainfall Events	Extreme Rainfall Events	Moderate Rainfall Events
Kendall's tau	0.000	0.170	0.213	-0.062
S	0.000	262.000	264.000	-103.000
Var(S)	22150.000	21654.667	16536.667	22221.667
p-value (Two-tailed)	1.000	0.046	0.041	0.494
alpha	0.050	0.050	0.050	0.050

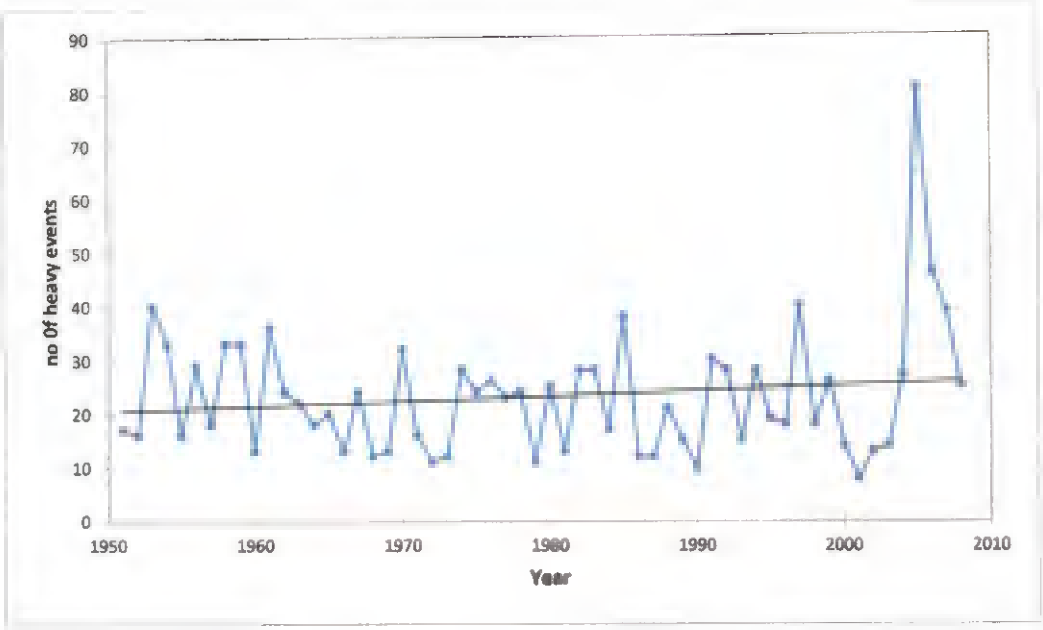

Figure 11. Temporal analysis of frequency of heavy rainfall events

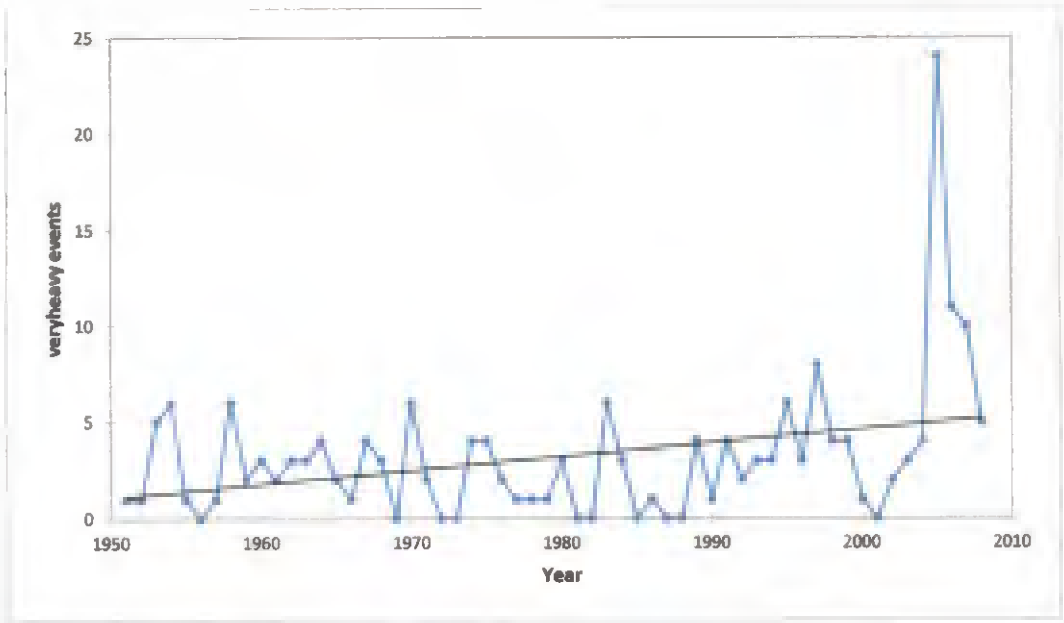

Figure 12. Temporal analysis of frequency of very heavy rainfall events

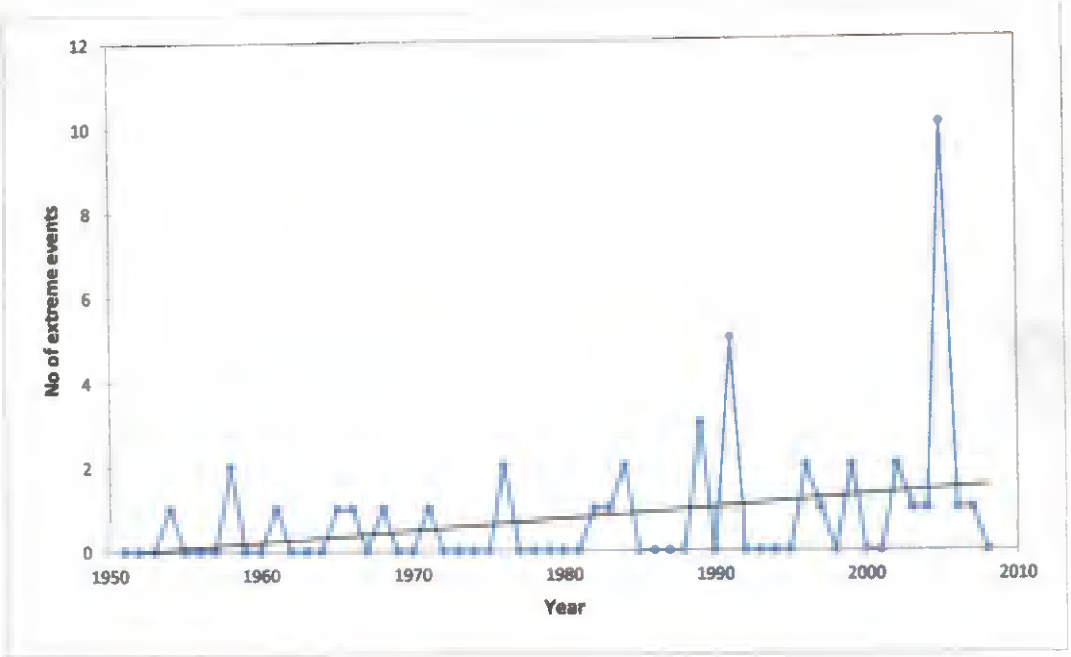

Figure 13. Temporal analysis of frequency of extreme rainfall events

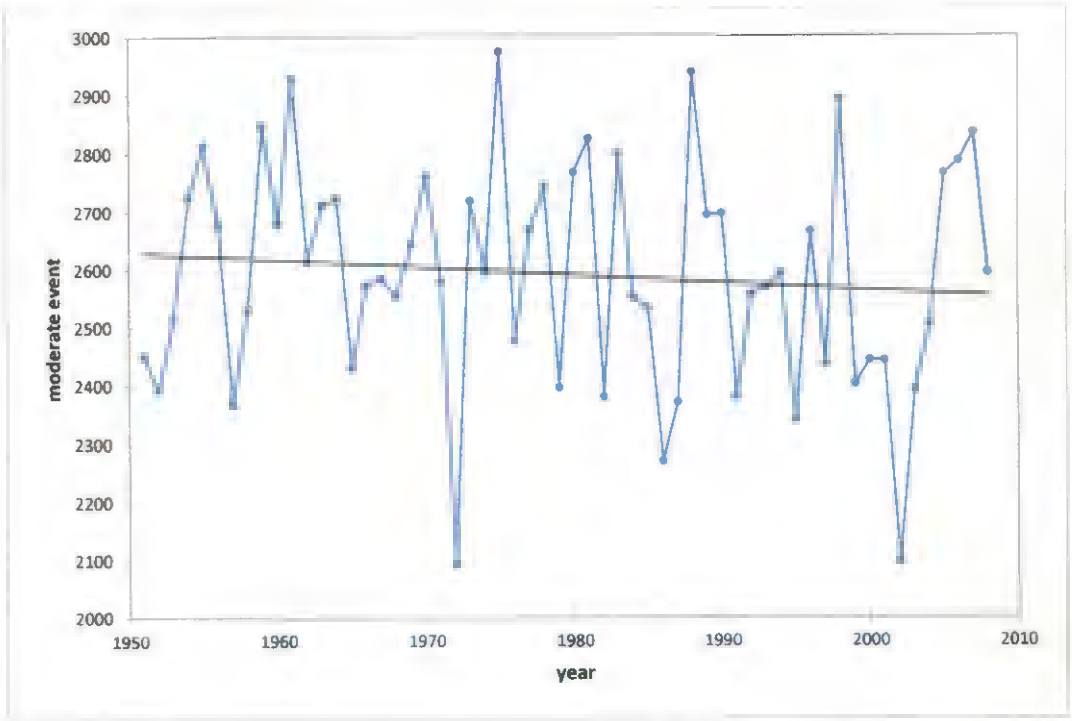

Figure 14. Temporal analysis of frequency of moderate rainfall events

4.3.3 Split period analysis

The Split Period trends in high intensity rainfall tries to capture the contrast in heavy and very heavy rainfall intensities during the initial and final period of 1951-1970 and 1989-2008 respectively.

4.3.3.1 Heavy rainfall events

The frequency analysis of the heavy rainfall events is represented on Figure14 and the statistical parameters are represented in Table 13.

The heavy rainfall events are seen to have decreasing trend in the initial period (not significant) and a rising trend in the latter period (significant).

4.3.3.2 Very heavy rainfall events

Figure 15 represents the trend analysis of very heavy rainfall events for the two periods. Mann Kendall Parameters of analysis are given on Table 13.

Both periods show a rising trend (not significant) but the trend line of the latter period is steeper implicating amore number of very heavy rainfall occurrences in the latter period of 1989-2008.

Thus, it can be concluded that the heavy rainfall events are found to have increased after the mid-eighties. A similar analysis conducted on the Narmada basin with 23 grids of the same dimension exhibited a different result. Significant rising trends were found in the latter period of both the events.

Table 13. Statistical Parameters of Mann Kendall Trend Analysis for frequency analysis of heavy and very heavy rainfall events for the periods of 1951-1970 and 1989-2008

	Heavy Rainfall Events		Very Heavy Rainfall Events	
	1951-1970	1989-2008	1951-1970	1989-2008
Kendall's tau	-0.189	0.128	0.146	0.277
S	-35.000	24.000	26.000	50.000
Var(S)	939.667	946.000	915.333	922.667
p-value (Two-tailed)	0.267	0.045	0.409	0.107
alpha	0.050	0.050	0.050	0.050

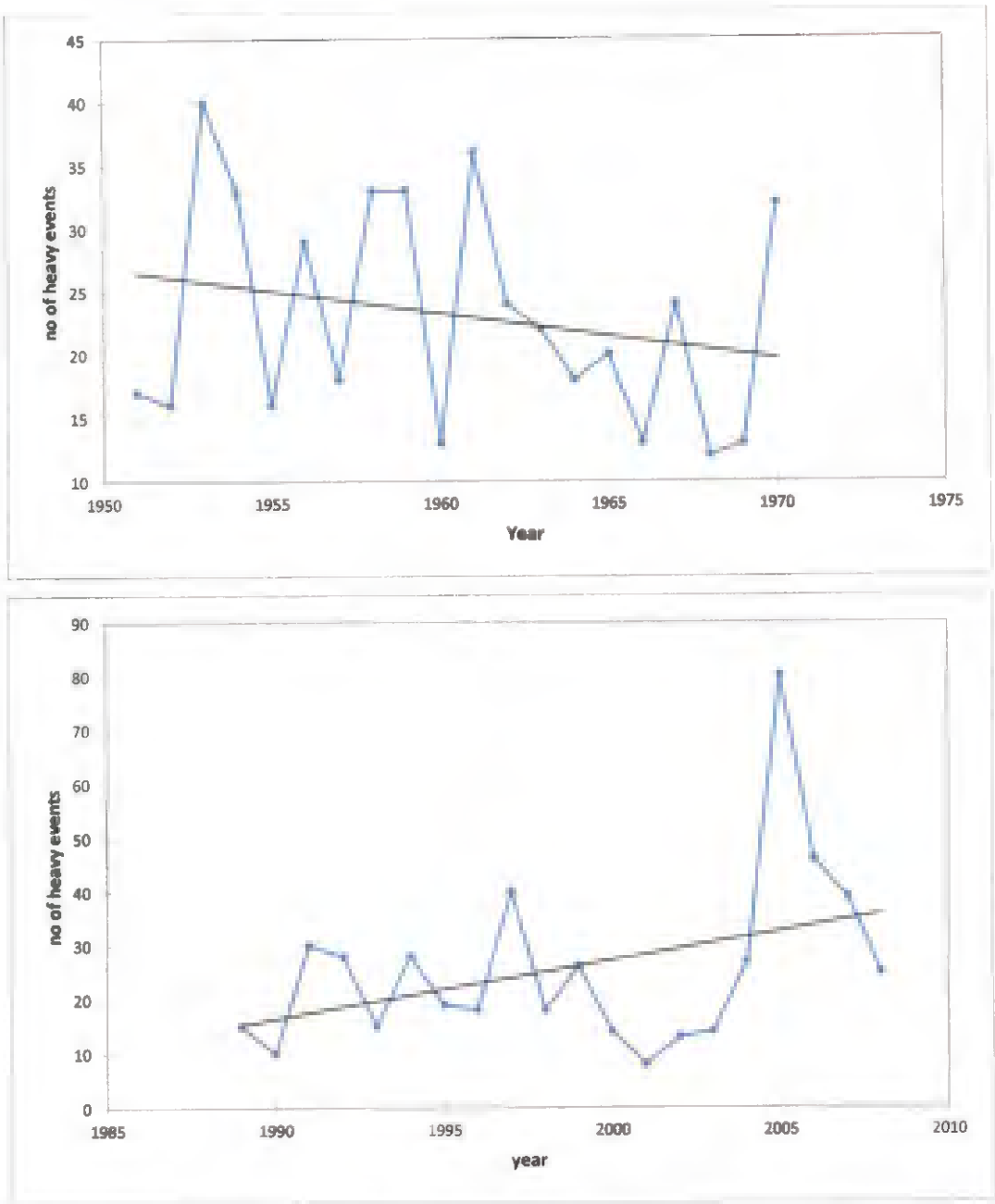

Figure 15. Temporal analysis of frequency of heavy rainfall events in split periods of 1951-1970 and 1989-2008.

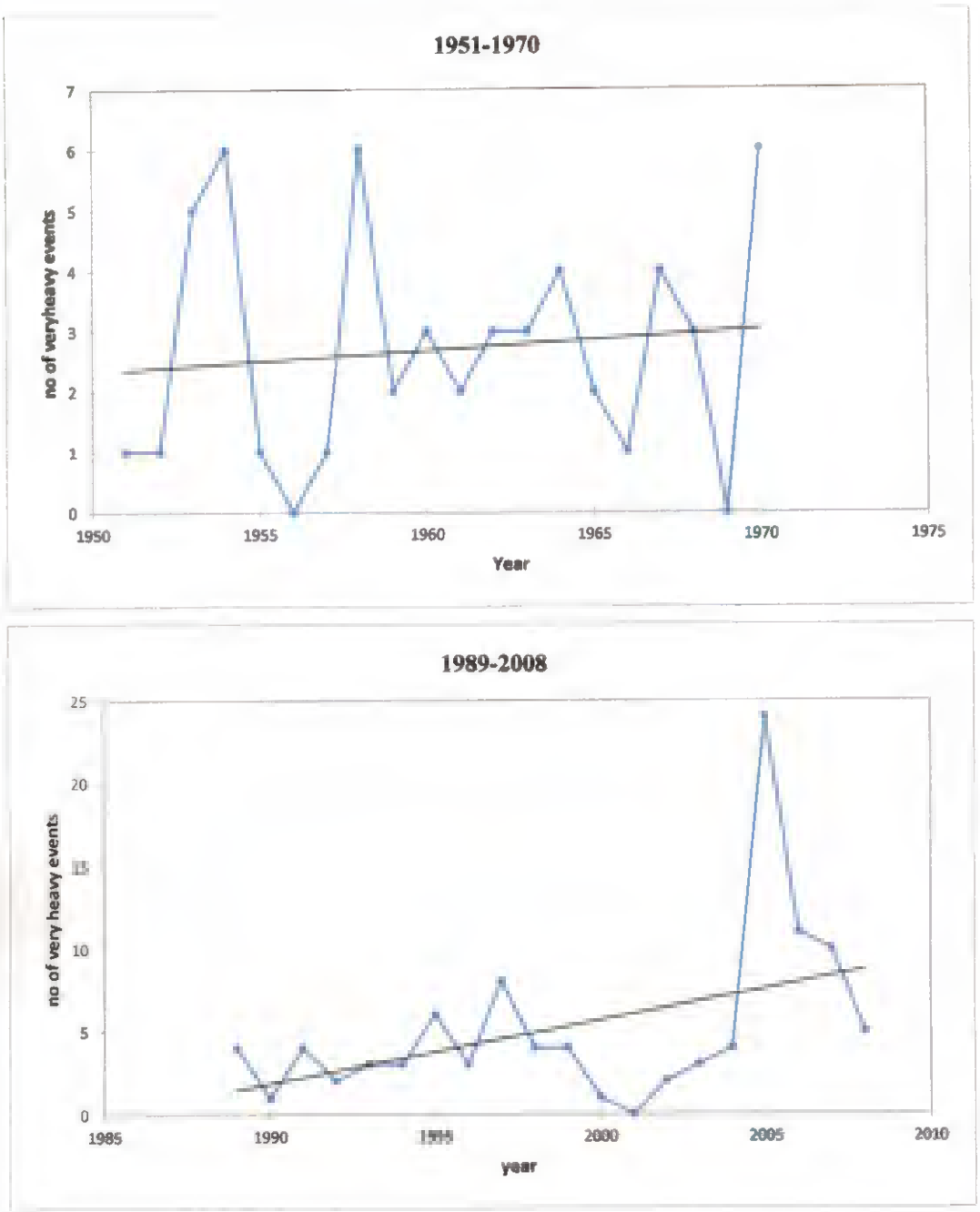

Figure 16. Temporal analysis of frequency of very heavy rainfall events in split periods of 1951-1970 and 1989-2008.

4.4 CONTRIBUTION OF MODERATE AND HIGH INTENSITY RAINFALL EVENTS TO THE ISMR MEAN

The contribution of Moderate events (>2.5 mm and <100mm) and high intensity events (>100mm) to the Indian Summer Monsoonal Rainfall over the Western Ghats Region is calculated for the split periods of 1951-1970 and 1989-2008. This could give a picture on the influence of the two types of rainfall events on the annual mean monsoonal rainfall and the shift that has occurred over the two periods.

The contribution of moderate and high intensity rainfall to the ISMR mean is given in Table 14. and Table 15. for the whole region and constituent grids respectively. The stacked area graph showing mean annual rainfall along with mean annual moderate rainfall and mean annual high intensity rainfall is given in Figure 17. The contribution of moderate and high intensity events to the annual mean can be understood from this graph. The increasing influence of high intensity rainfall to the annual mean can be seen over the years.

Contribution of moderate rainfall to the ISMR mean was 92.19 per cent in the former period which decreased to 90.13 per cent in the latter period. A decrease of 2.06 per cent has occurred. High Intensity rainfall events contributed to 8.1 per cent of the mean in the latter period compared to 6.1 per cent in the earlier period. An increase of 2 per cent has occurred in the share of high intensity rainfall.

Grid wise analysis of contribution of the two types of rainfall to the ISMR mean indicates that out of 32 grids, 26 grids have an increase in high intensity rainfall events and 23 grids show decreasing shares of moderate rainfall when the two-time periods are considered. The highest increase in high intensity rainfall is seen in grids 393 (7.23%) followed by 428 (6.52%) and 463 (5.3%). The grid 393 exhibited the largest decrease in moderate rainfall with a magnitude of increase of 7.16 per cent. It was observed in grid 393 that the increase in heavy rainfall has occurred almost entirely at the expense of moderate rainfall.

Goswami *et.al.*, (2006) in his study to examine the extreme events over India had found out that the relative contributions to the mean from the two classes of rainfall namely, high intensity events and moderate events, balance in a given year in Central India. The contribution from the decreasing trend of moderate events is partially offset by that from increasing heavy rain events. Consequently, the seasonal total does not show any statistically significant change over longer time scales. This notion can be applied in the current research as the seasonal mean here too does not show a trend. The mean nullifies the effect of reduced moderate intensity events by compensating with the contribution from high intensity rainfalls.

Table 14. Share of moderate and high intensity rainfall events to the annual monsoonal mean rainfall during the periods 1951-1970 and 1989-2008 for Western Ghats.

Initial 20-year period (1951-1970)		Final 20-year period (1989-2008)	
moderate rainfall	High Intensity Rainfall	moderate rainfall	High Intensity Rainfall
92.19%	6.09 %	90.13 %	8.12%

Table 15. Share of moderate and high intensity rainfall events to the annual monsoonal mean rainfall during the periods 1951-1970 and 1989-2008 for Constituent Grids of Western Ghats

Grid	Initial 20-year period (1951-1970)		Final 20-year period (1989-2008)	
	moderate rainfall	heavy rainfall	moderate rainfall	heavy rainfall
81	95.72	0.00	95.57	0.00
115	97.07	1.92	96.27	2.57
116	95.66	0.52	95.67	0.62
117	81.26	0.00	85.40	2.35
150	98.01	1.08	96.12	2.53
151	95.72	0.00	94.25	1.42
152	84.01	0.00	85.29	5.35
184	90.28	9.28	91.02	8.43
185	98.52	0.56	96.55	2.42
186	92.31	0.00	90.13	2.96
219	92.18	7.42	92.92	6.64
220	97.88	0.35	96.58	1.86
253	84.45	15.18	84.12	15.50
254	97.76	1.63	94.67	4.60
255	92.70	0.00	91.00	3.61
288	95.40	3.98	91.42	7.83
289	98.15	0.41	95.14	3.10
323	97.87	1.14	94.98	3.92
324	93.63	0.00	92.82	1.60
357	79.59	20.0	81.84	17.66
358	97.4	1.47	95.90	2.89
359	86.2	0.00	90.15	0.00
392	84.19	15.30	79.55	19.85
393	96.30	2.49	89.14	9.72
394	88.16	0.00	90.51	2.54
427	87.98	11.28	83.55	15.65
428	96.40	2.04	90.06	8.56
429	90.64	0.00	90.87	2.42
462	89.04	10.01	83.74	15.05
463	96.44	1.60	90.97	6.90
497	92.79	5.23	87.15	10.53
498	93.18	3.61	91.62	4.85

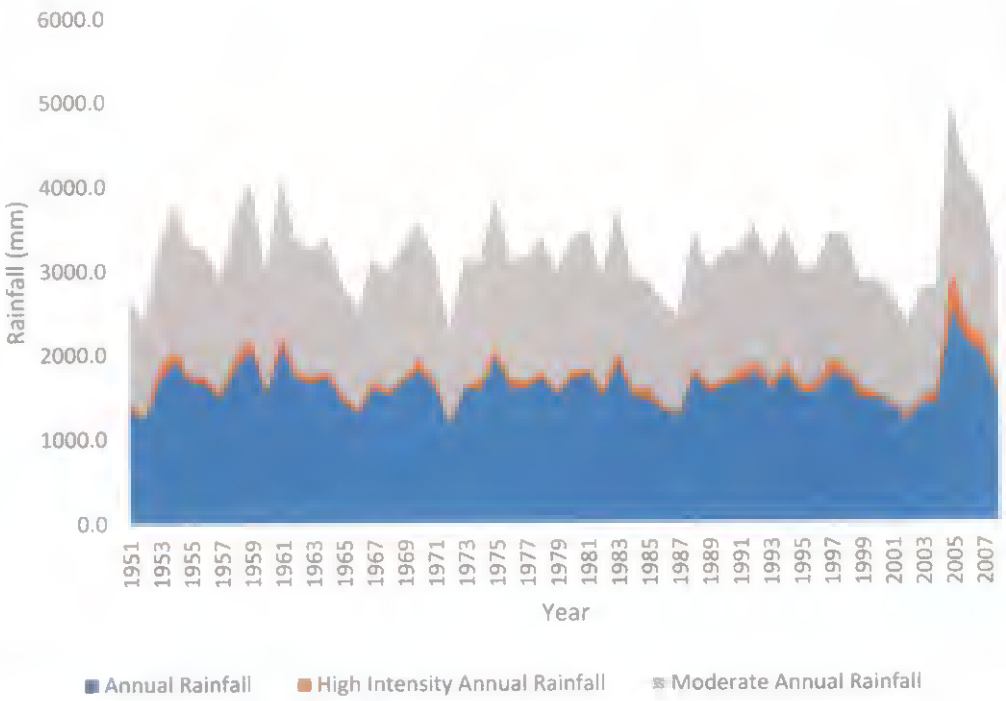

Figure 17. Stacked area chart showing mean annual rainfall, mean annual moderate rainfall and mean annual high intensity rainfall.

4.5 RETURN PERIOD ANALYSIS

The aim of this section is to model the occurrence of daily extreme precipitation values (one day maximum rainfall) by employing the Generalized Extreme Value (GEV) distribution of the Extreme Value Theory. The GEV goodness of fit is evaluated by quantile–quantile (Q-Q) plot and by the application of the Kolmogorov–Smirnov (KS) test, which compares the cumulated empirical distributions with the theoretical ones. The graphical Q-Q plot suggests that the probability distributions of the studied series are appropriated, and these results were confirmed by the empirical KS test.

The first step in modelling the Return Level is to create the daily extreme rainfall data out of the total ISMR series. The independence and homogeneity of data is checked using the Run's test. For the whole region, the runs test was calculated at 5 per cent significance and the data was found to be independent. The P value is higher than 0.05. Similar results are obtained for all the constituent grids. The statistical parameters of the Run's test are given in Table 16.

After fitting the GEV distribution, the μ, σ and ξ values are calculated (location, scale and shape parameters respectively). The Return Levels are extracted out of the probability plots. The return levels for specific return periods (2, 5, 10, 25, 50 and 100 years) for both the entire region and the constituent grids are obtained and tabulated on tables, Table 17 and Table 18. The Probability plot based on the return period quantiles are plotted as shown in Figure 18.

To test the Goodness of fit of the distribution, the Q-Q plot was plotted which is represented in Figure 19. The figures show that most of the points of Q-Q plot are located near the diagonal (45°) line, suggesting that the chosen and fitted theoretical distributions are appropriate. To further support these results, the KS test was calculated. The KS value was found to be satisfactory (Dn = 0.0987) and conforming to the q-q plot analysis.

The 2 year, 5 year, 10year, 25 year, 50 year and 100 year return levels of rainfall are found to be 186.2mm, 224.3 mm, 250.2 mm, 283.8 mm, 309.3 mm and 335.1 mm.

The return levels for the two-year return period were seen to be over 100 mm for the grids of 184 (118mm), 219 (114.9mm), 253 (145.8mm), 285 (104.5mm), 357 (147.6 mm), 392 (144.2mm), 427 (129.9mm) and 462 (122.4mm).

The grids with highest two-year return levels are 357, 253 and 392 with 147.6mm, 145.8 mm and 144.2 mm respectively. The grids with the lowest two-year return periods are 117 and 152 with 19.4mm and 24.2 mm respectively.

The probability plots of the 32 constituent grids based on the return period quantiles are represented in Figure 20.

The return periods of extreme rainfall events of the Western Ghats have not been much explored and a grid based approach for modelling return period values is fairly new. A station based analysis cannot often reveal the underlying frequency whereas a grid based research can give a generalized insight into the rainfall frequencies over the years overcoming the inherent variabilities in localized rainfalls.

Frequency analysis of annual one day maximum rainfall at Amman Zarqa Basin, Jordan was carried out (Al-Houri *et.al.*, 2014) to find out return period levels of extreme rainfall events using data from 22 stations. The distributions used for fitting the curves of maximum rainfall values were namely: Linear and log normal distributions. The goodness of fit for the selected distributions is tested using the Chi-square and the Kolmogorov–Smirnov tests. Frequency analysis was then conducted to extract the magnitude of one day annual maximum rainfall corresponding to 2, 5, 10, 25, 50 and 100-year return periods as in this case for the 22 stations in AZB.

A return period analysis of one day maximum rainfall in the context of India was done in Punjab using 38 years of precipitation data for the station of Ludhiana (Kumar and Bhardwaj, 2015). Three probability distributions such as Log Normal,

Gumbel and Log Pearson Type-III distribution were used to determine the best fit probability distribution that describes the annual one day maximum rainfall by comparing with the Chi-square value wherein Log Pearson Type-III distribution was found to be the best fit. It was found that the maximum of 373.42 mm rainfall could be received with 25 years return period.

The seasonal analysis of return periods of one day maximum rainfalls of the Brazilian Amazon (Santos *et.al.*, 2016) was carried out using distributions of Generalized Extreme Value distribution and Generalized Pareto Distributions using the data from 1983-2012. The GPD uses a percentile approach to extract out extreme values whereas the GEV method uses a fixed threshold approach. The GEV method however was seen to be the best fit relative to the GPD. The GPD was not used in the current study and the GEV distribution alone was employed.

The performed regional analyses of daily precipitation extreme events in the Western Ghats are expected to contribute to better strategic planning and minimize the risk of losses in productive sectors (particularly in agriculture and electric power generation and distribution). Analysis of rainfall regime would enhance the management of water to prevent floods and droughts as well as an effective design of drainage structures especially in relation to their required hydraulic capacity.

Table 16. Statistical Parameters of the Run's test conducted on the ODMR values over the study area

R	25.000
r Expected value	29.138
p-value (Two-tailed)	0.321
Alpha	0.050

Table 17. Return Levels of daily extreme precipitation for specific return periods in the Western Ghats

Return Period	2 year	5 year	10 year	25 year	50 year	100 year
Return Levels (mm)	186.2	224.3	250.2	283.8	309.3	335.1

Table 18. Return Levels of daily extreme precipitation for specific return periods in the Western Ghats for its constituent grids

grid	return levels (mm)					
	2 year	5 year	10 year	25 year	50 year	100 year
81	45.5	58.0	65.4	73.9	79.6	84.8
115	80.7	100.7	113.9	130.5	142.8	155.0
116	40.1	48.2	52.4	56.6	59.0	61.0
117	19.4	26.7	30.8	35.2	38.0	40.5
150	81.4	103.3	119.1	140.7	158.1	176.5
151	44.3	57.6	65.8	75.6	82.4	88.9
152	24.2	31.9	36.3	41.0	44.1	46.8
184	118.0	155.3	187.0	237.3	283.8	339.4
185	79.3	103.2	120.7	145.1	164.9	186.1
186	36.4	48.3	55.5	64.0	69.7	75.1
219	114.9	146.9	172.3	210.1	243.1	280.6
220	61.1	77.2	87.2	99.0	107.4	115.2
253	145.8	174.0	191.4	212.0	226.3	239.8

254	91.2	111.1	123.7	138.8	149.6	159.9
255	36.3	46.9	53.1	60.0	64.5	68.6
288	104.5	122.5	132.0	142.1	148.2	153.4
289	61.4	74.2	81.4	89.1	94.0	98.2
323	83.4	98.6	107.3	116.9	123.1	128.6
324	42.6	53.3	59.5	66.5	71.2	75.4
357	147.6	191.0	224.2	272.2	312.6	357.3
358	84.5	112.3	135.6	172.1	205.3	244.7
359	33.0	46.4	55.6	67.8	77.2	86.9
392	144.2	181.0	205.2	235.6	258.1	280.4
393	87.0	110.0	124.4	141.9	154.2	166.1
394	33.9	43.7	48.6	53.3	56.0	58.2
427	129.9	152.7	165.1	178.3	186.5	193.5
428	80.0	101.1	113.2	126.9	135.9	143.9
429	32.6	40.9	44.8	48.5	50.5	52.1
462	122.4	155.2	176.7	203.4	222.9	242.1
463	76.5	96.7	108.5	121.6	130.3	138.0
497	92.8	119.2	134.6	151.9	163.4	173.8
498	74.1	103.5	123.9	150.9	171.9	193.5

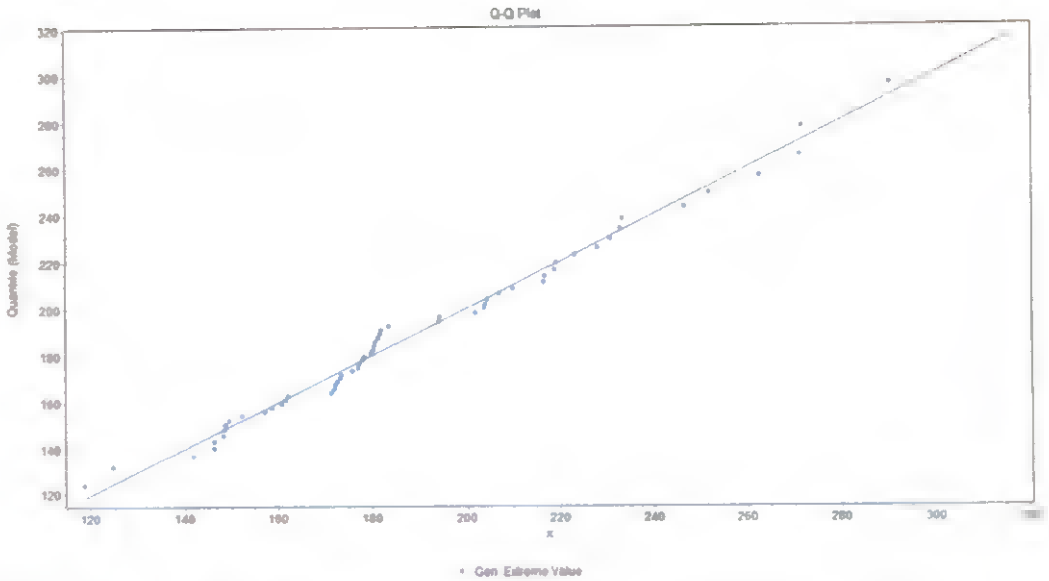

Figure 18. Q-Q plot

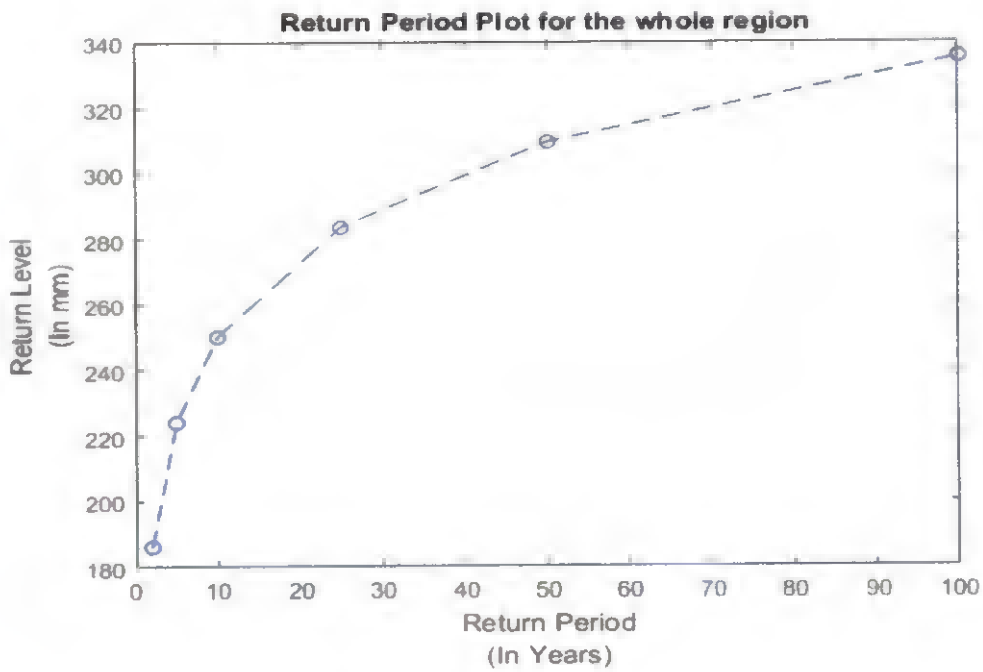

Figure 19. Return period plot for the whole region

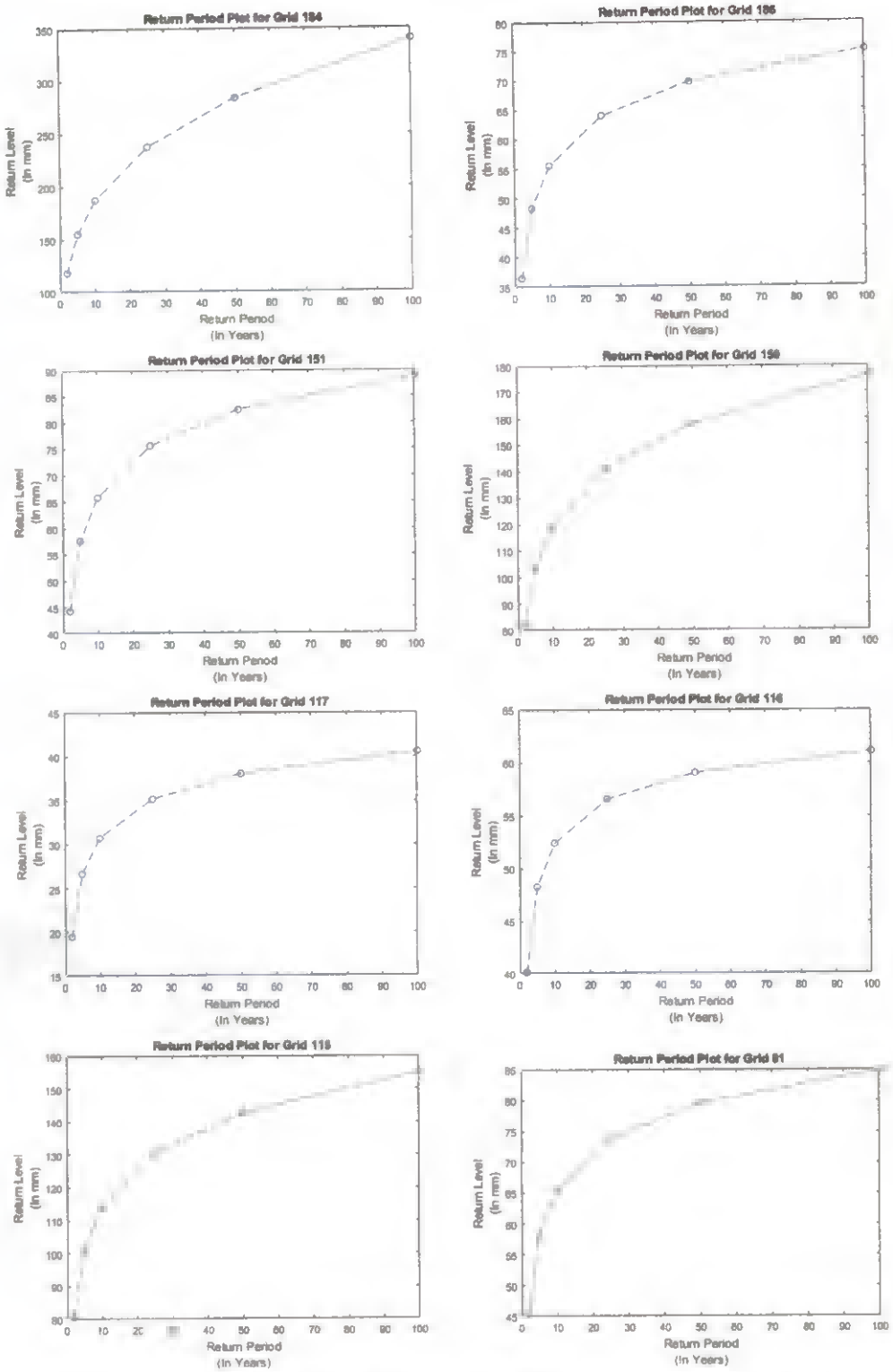

Figure 20a. Probability plots of the grids (81, 115, 116, 117, 150, 151, 152 and 184) based on the return period quantiles.

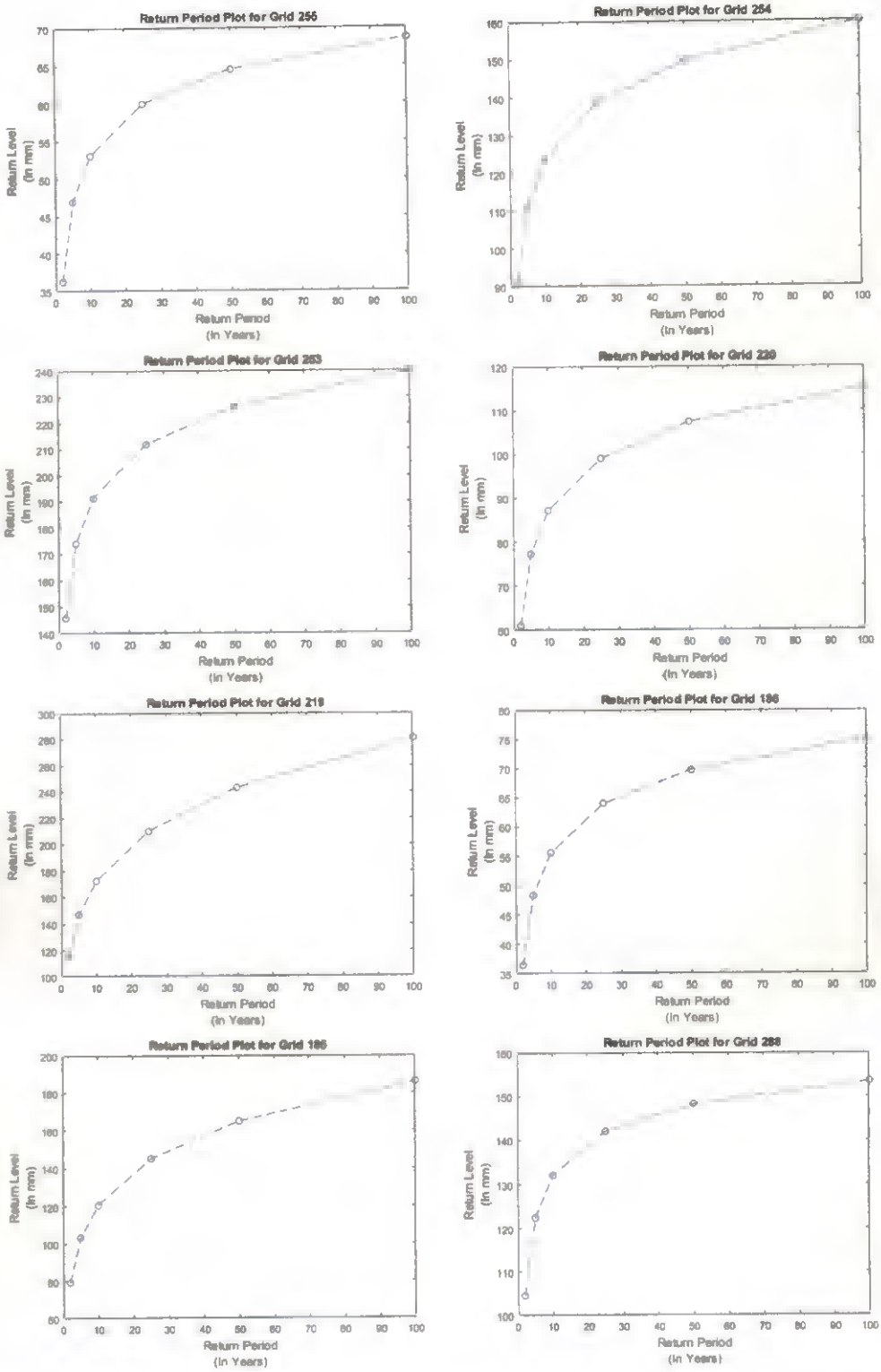

Figure 20b. Probability plots of the grids (185, 186, 219, 220, 253, 254, 255 and 288) based on the return period quantiles.

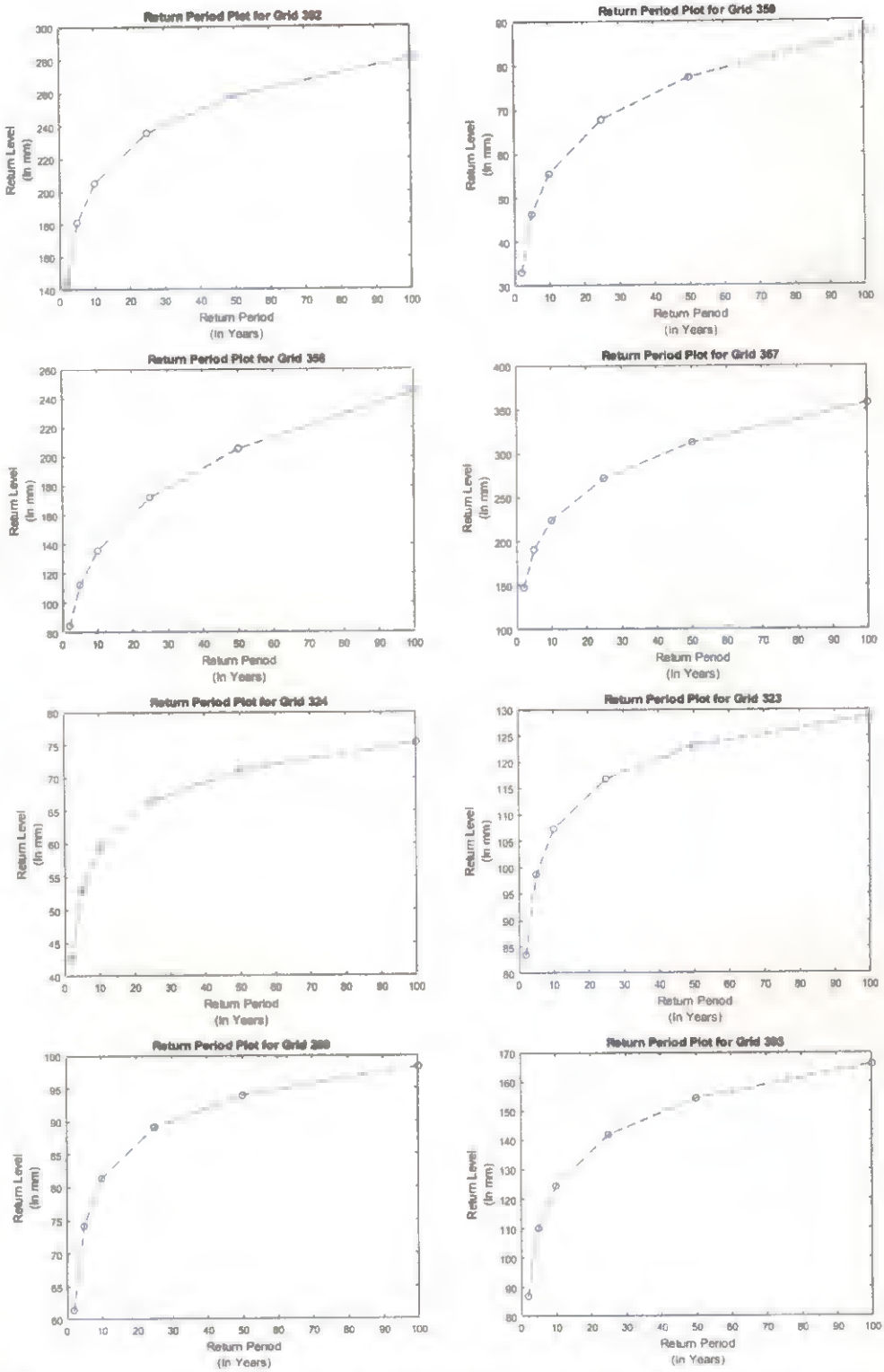

Figure 20c. Probability plots of the grids (289, 323, 324, 357, 358, 359, 392 and 393) based on the return period quantiles.

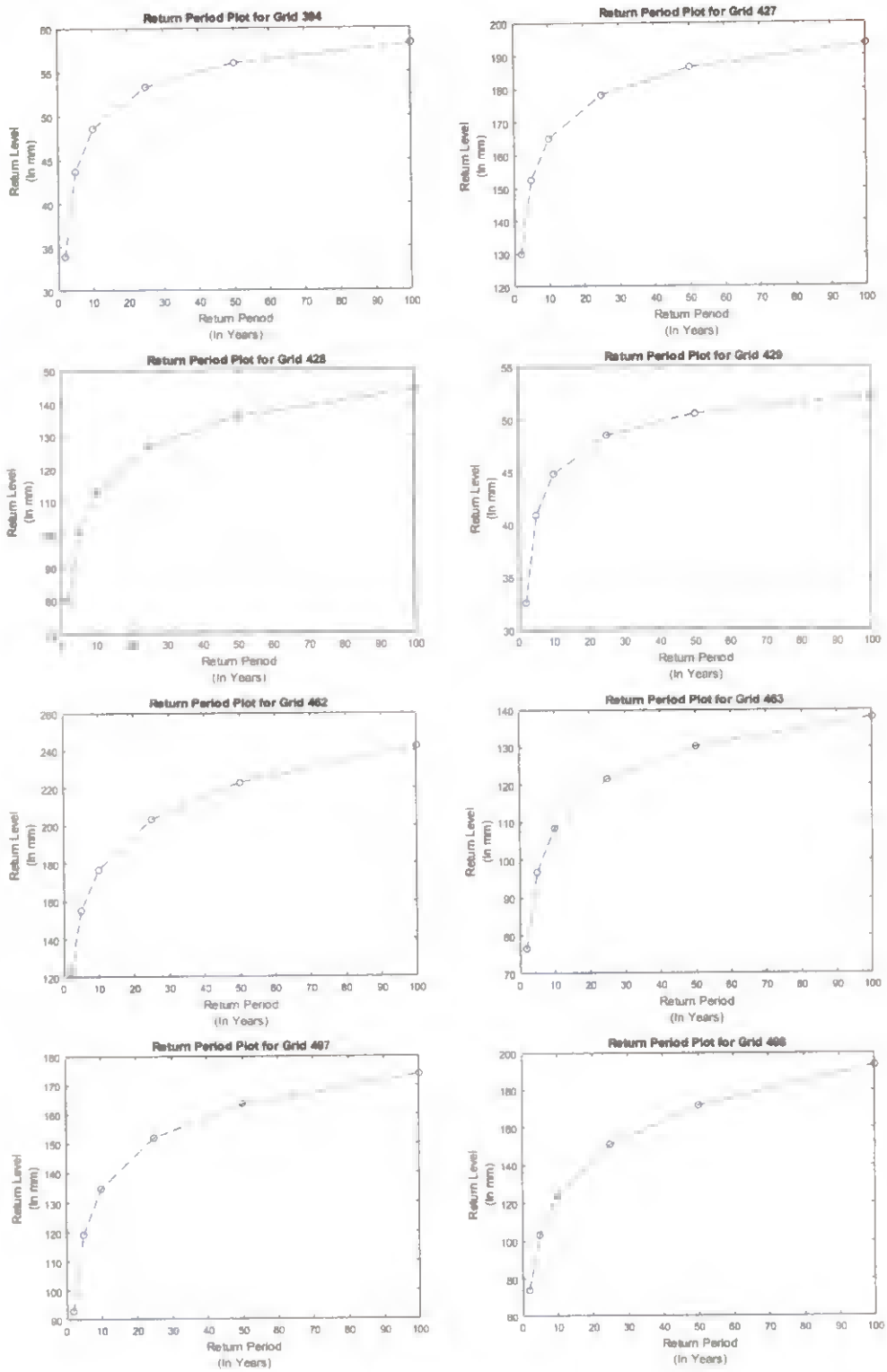

Figure 20d. Probability plots of the grids (394, 427, 428, 429, 462, 463, 497 and 498) based on the return period quantiles.

CHAPTER 5

SUMMARY AND CONCLUSION

Western Ghats, identified as one of India's largest natural carbon sinks and a biodiversity hotspot occupies a strategic location along the incoming monsoonal track of India. The Ghats with its strategic position plays a great role in channelling the summer monsoonal rain into the mainland. The area encompassed by the Ghats and the coast through its topography, vegetation and orographic effect forms a region with unique climatology. The natural ecosystems and human livelihoods of this region are highly dependent on the Indian Summer Monsoon rainfalls and even the slightest change can trigger a change in these systems. The global climate changing scenario is having its toll in the monsoonal system. Uncertainties in Rainfall has been a major issue and studies have shown that there has been a decrease in the summer monsoon rainfall (Ghosh *et al.,* 2009) and an increase in hot days with subsequent decrease in cold nights over the region for the period from 1971 to 2005.

According to Goswami *et.al.*, (2006) there has been a significantly increasing trend in the frequency and magnitude of extreme events and a significantly decreasing trend in the frequency of moderate events over Central India during the monsoon seasons from 1951 to 2000. The western Ghats being spread over a large region, instances of extreme and moderate events may occur simultaneously and the significance of these events needs to be assessed and it needs to be understood whether the processes occurring are out of sheer climatic chaos associated with the noisy monsoon system or if it is a product of well-defined climatic trends.

The objective of the research was to identify the trends in Indian Monsoonal Rainfall over the study area of the Western Ghats. The study area included the area from the Ghats up to the coast. The data that has been used for the analysis is the $1^0 \times 1^0$ data for the Rainfall over India for the period 1951-2008. The trends in extreme events were given a special emphasis. Both Regional and constituent grid

analysis was done. The parameters that are analyzed for were One Day Maximum Rainfall (ODMR), which is the maximum precipitation magnitude in a given day (24 hours) in a given season (South West Monsoonal Season here) and high intensity rainfall events. High Intensity Rainfall events are heavy rainfall events (>100m and <150mm), very heavy rainfall events (>150mm and <200mm) and extreme events (>200mm). The frequency analysis in terms of distribution of these trends in grids and its occurrence frequency has been done for the whole period and for sub periods of 1951-1970 and 1989-2008 to capture the contrast in events that has occurred in the recent decades.

The trends in this research were analyzed using Mann Kendall method of trend analysis which is a non-parametric method for assessing trends. The shift in dates of the ODMR too has been calculated along with the contribution of moderate and high intensity rainfalls to the ISMR annual mean. The final parameter was to model the return periods of the daily maximum extremes or ODMR using the Generalized Extreme Value Theory of the Extreme Value Theorem. Probability plots were drawn representing the return periods and Return levels for different grids and also for the whole region. The goodness of fit was ascertained by using graphical method of Quantile-Quantile Plot and empirical method of Kolmogorov Smirnov test.

Salient findings of the Research are briefed below:

- The mean annual monsoonal rainfall over the study area is 1616.15 mm and the standard deviation is 242.966.
- It is observed that the mean annual monsoonal rainfall varies from 231.4 mm in grid 117 to 3416 mm in grid 253.
- The one day maximum rainfall extracted from the 32 constituent grids for the entire period showed a variation from 118.63 mm in 1981 to 316.63 mm in 2005.
- The temporal variation in one day maximum rainfall for the time series is having a significant trend. The values are seen to be increasing steadily and a profound increase is observed in the recent few decades.

- When the One day maximum rainfall was analysed for the latitudes, two latitudes (14° and 21°N were seen to have significant positive trends in One Day Maximum Rainfall in the whole region.
- There are 7 grids (186, 359, 394, 428, 429, 497 and 498) out of the 32 grids which show a significant rising trend in one day maximum rainfall.
- It has been observed from the table that during the recent few years, the occurrence of One day maximum Rainfall has shifted to the far end of the season as in years 2006 and 2008 respectively when the ODMR occurred on the 98th and 72nd day respectively.
- A significant trend has been seen in the increase in number of grids getting heavy, very heavy and extreme rainfall events.
- No significant trend observed in the instances of heavy rainfall over the years but significant trend observed in the occurrences of events of very heavy and extreme magnitudes.
- Even though a negative trend is observed in the occurrence of moderate rainfall over the years, no significant trend has been found.
- When split period analysis of the contribution of moderate and high intensity rainfalls were observed, the share of high intensity rainfalls were seen to increase and a decrease was observed in the share of moderate events.
- The return period analysis of the one day maximum rainfall events has been done and it was observed that the 2 year, 5 year, 10year, 25 year, 50 year and 100 year return levels of rainfall are found to be 186.2mm, 224.3 mm, 250.2 mm, 283.8 mm, 309.3 mm and 335.1 mm for the complete region.
- The return levels for the two year return period are seen to be over 100 mm for the grids of 184 (118mm), 219 (114.9mm), 253 (145.8mm), 285 (104.5mm), 357 (147.6 mm), 392 (144.2mm), 427 (129.9mm) and 462 (122.4mm).

The one day maximum rainfall trend in the Western Ghats was found to have a significant rising trend. The ecological, economic, and social impacts that could result if increasing precipitation trends continue in the region in the future could

depend on these extreme events. For coastal areas, in particular tropical storms, and coastal storms form a major hazard. The vulnerability to storms might further be aggravated if extreme rainfall episodes continue in the future and consequently result in inland and coastal flooding. Institutional changes, coastal regulation, and management goals have to be, therefore, adapted in a timely manner.

REFERENCES

Al-Houri, Z., Al-Omari, A., and Saleh. O. 2014. Frequency analysis of annual one day maximum rainfall at Amman Zarqa Basin, Jordan. *Civil Environ. Res.* 6 (3): 44-57.

Bedient, P. B. and Huber W. C. 1948. *Hydrology and Flooding Analysis*. Addison Wesley Publishing Co. 158p.

Bhaskar, S. R., Bansal, A. N., Chhajed, N., and Purohit, R. C. 2006. Frequency analysis of consecutive days maximum rainfall at Banswara, Rajasthan, India. *J. Engg. Appl. Sci.* 1 (3): 64-67.

Bhattacharya, A. K. and Sarkar, T. K. 1982. Analysis of rainfall data for Agricultural land drainage design. *J. Agricul. Engg.* 33 (3): 269-284.

Boos, W. R. and Emanuel, K. A. 2009. Annual intensification of the Somali jet in a quasi-equilibrium framework: Observational composites. *Q. J. R. Meteorol. Soc.* 135: 319–335.

Boos, W. R. and Kuang, Z. 2010. Dominant control of the South Asian monsoon by orographic insulation versus plateau heating. *Nat.* 463: 218-222.

Bordoni, S. and Schneider, T. 2008. Monsoons as eddy-mediated regime transitions of the tropical overturning circulation. *Nat. Geosci.* 1: 515–519.

Chakravarti, I. M., Laha, R. G., and Roy, J. 1967. *Handbook of Methods of Applied Statistics: Vol. 1.* John Wiley and Sons, UK, pp.392–394.

Charney, J. G. and Shukla, J. 1981. Predictability of monsoons. In: Lighthill, J. and Pearce, R. P. (eds), *Monsoon Dynamics*. Cambridge University Press, Cambridge, pp.99-109.

Chou, C. 2003. Land-sea heating contrast in an idealized Asian summer monsoon. *Clim. Dynam.* 21: 11–25.

Coles, S. 2001. *An Introduction to Statistical Modeling of Extreme Values*. Springer, London, 209p.

Easterbrook, D. and D'Aleo, J. 2011. Relationship of multidecadal global temperatures to multidecadal oceanic oscillations. *Evidence-Based Climate Sci.* 161-184.

Fasullo, J. and Webster, P. J. 2003. A hydrological definition of Indian monsoon onset and withdrawal. *J. Clim.* 16: 3200–3211.

Findlater, J. 1969. A major low-level air current near the Indian Ocean during northern summer: Inter hemispheric transport of air in the lower troposphere over western Indian Ocean. *Q. J. R. Meteorol. Soc.* 96: 551–554.

Fisher, R. A. and Tippett, L. H. C. 1928. Limiting forms of the frequency distribution of the largest or smallest member of a sample. *Proc. Camb. Philos. Soc.* 24 (2): 180–190.

Ghosh, S., Luniya, V., and Gupta, A. 2009. Trend analysis of Indian summer monsoon rainfall at different spatial scales. *Atm. Sci. Let.* 10 (4): 285-290.

Goswami, B. N., Venugopal, V., Dengupta, D., Madhusoosanan, M. S., and Xavier, K. P. 2006. Increasing trend of extreme rain events over India in a warming environment. *Sci.* 314: 1442–1445.

Groisman, P. Y., Karl, T. R., Easterling, D. R., Knight, R. W., Jamason, P. F., Hennessy, K. J., Suppiah, R., Page, C. M., Wibig, J., Fortuniak, K., Razivaev, V. R., Douglas A., Forland, E., and Zai, P. 1999. Changes in the probability of heavy precipitation: Important indicators of climatic change. *Clim. Change*, 42: 243–283.

Guhathukurta, P. and Rajeevan, M. 2008. Trends in rainfall pattern over India. *Int. J. Clim.* 28 (11): 1453-1470

Hamed, K. H. and Rao, A. R. 1998. A modified Mann-Kendell trend test for autocorrelated data. *J. Hydrol.* 204 (1): 182-196.

Hoskins, B. J. and Rodwell, M. J. 1995. A model of the Asian summer monsoon. Part 1: The global scale. *J. Atmos. Sci.* 52: 1329–1340.

IPCC [Intergovernmental Panel on Climate Change]. 2007. *Adaptation and mitigation options*. Fourth Assessment Report Climate Change. [on-line]. Available: https://www.ipcc.ch/pdf/assessment-report/ar4/wg2/ar4_wg2_ full report. pdf (15 June 2016).

IPCC [Intergovernmental Panel on Climate Change]. 2013. *Climate Change 2013: The Physical Science Basis.* Available: http://www.climatechange2013.org/images/report/WG1AR5_ALL_FINA L.pdf. [29 May 2015].

IPCC [Intergovernmental Panel on Climate Change]. 2014. *Climate Change 2014: A SynthesisReport.* [On-line]. Available: http://www.ipcc.ch/pdf/ assessment_report/ar5/syr/AR5_SYR_FINAL_All_Topics.pdf [29 May 2015].

Jeevrathnam, K. and Kumar, J. 1979. Probability analysis of maximum daily rainfall for Ootacamud. *Indian J. Soil Cons.* 7 (1): 10-16.

Jenkinson, A. F. 1955. The frequency distribution of the annual maximum (or minimum) of meteorological elements. *Q. J. R. Meteorol. Soc.* 81: 158–171.

Jha, C. S., Dutt, C. B. S., and Bawa, K. S. 2000. Deforestation and land use changes in Western Ghats, India. *Curr. Sci.* 79 (2): 231-238.

Kharin, V. V. and Zwiers, F. W. 2000. Changes in the extremes in an ensemble of transient climate simulations with a coupled atmosphere–ocean GCM. *J. Clim.* 13: 3760–3788.

Kumar, R. K., Pant, G. B., Parthasarathy, B., and Sontakke, N. A. 1992. Spatial and sub-seasonal patterns of the long term trends of Indian summer monsoon rainfall. *Int. J. Climatol.* 12: 257– 268.

Kumar, A. and Bhardwaj, A., 2015. Probability analysis of return period of daily maximum rainfall in annualdata set of Ludhiana, Punjab. *Indian J. Agri.* 49 (2): 160-164.

Kumar, V. and Jain, S. K., 2010. Trends in seasonal and annual rainfall and rainy days in Kashmir valley in the last century. *Quaty. Int.* 212: 64–69.

Kumar, V., Jain, S. K., and Singh, Y. 2010. Analysis of long-term rainfall trends in India. *Hydrol. Sci. J.* 55: 484–496.

Kwaku, X. S. and Duke, O. 2007. Characterization and frequency analysis of one day annual maximum and two to five consecutive days maximum rainfall of Accra, Ghana. *J. Engg. Appl. Sci.* 2 (5): 147-153.

Li, C. F. and Yanai, M. 1996. The onset and inter-annual variability of the Asian summer monsoon in relation to land sea thermal contrast. *J. Clim.* 9: 358–375.

Loschnigg, J. and Webster, P. J. A. 2000. Coupled ocean-atmosphere system of SST modulation for the Indian Ocean. *J. Clim.* 13: 3342–3360.

Lucio, P.S. 2004. Assessing HadCM3 simulations from NCEP reanalyses over Europe: diagnostics of block-seasonal extreme temperature regimes. *Glob. Planet Chang.* 44: 39–57.

Manjunatha, B. R., Balakrishna, K., Krishnakumar, K. N., Manjunatha, H. V., Avinash, K. A., Mulemane, C., and Krishna, K. M. 2015. Increasing trend of rainfall over Agumbe, Western Ghats, India in the scenario of global warming. *Open Oceanogr. J.* 8: 39-44.

Maraun, D., Rust, H. W., and Osborn, T. J. 2009. The annual cycle of heavy precipitation across the United Kingdom: a model based on extreme value statistics. *Int. J. Climatol.* 29: 1731–1744.

Meehl, G. A. 1987. The annual cycle and interannual variability in the tropical Pacific and Indian-Ocean regions. *Mon. Weath. Rev.* 115: 27–50.

Onoz, B. and Bayazit, M. 2012. The Power of Statistical Tests for Trend Detection. *Turkish J. Eng. Environ. Sci.* 27: 247 – 251.

Pal, I. and Al-Tabbaa, A. 2011. Assessing seasonal precipitation trends in India using parametric and non-parametric statistical techniques. *Theor. Appl. Climatol.* 103: 1–11.

Palutikof, J. P., Brabson, B. B., Lister, D. H., and Adcock, S. T. 1999. A review of methods to calculate extreme wind speeds. *Meteorol. Appl.* 6 (2): 119– 132.

Pant, G. B. and Hingane, L. S. 1988. Climatic changes in and around the Rajasthan desert during the 20th century. *Int. J. Climatol.* 8: 391–401.

Parthasarathy, B. and Dhar, O. N. 1974. Secular variations of regional rainfall over India. *Q. J. R. Meteorol. Soc.* 100: 245–257.

Prakash, V, S., Mahesh, S. C., and Gairola, R. M. 2013. Is summer monsoon rainfall over the west coast of India decreasing? *Atmos. Sci. Let.* 14: 160–163.

Prive, N. C. and Plumb, R. A. 2007. Monsoon dynamics with interactive forcing. Part I: Axisymmetric studies. *J. Atmos. Sci.* 64: 1417–1430.

Rajeevan, M., Bhate, J., and Jaswal, A. K. 2008. Analysis of variability and trends of extreme rainfall events over India using 104 years of gridded daily rainfall data. *Geophys. Res. Lett.* 35 (18).

Rajeevan, M., Bhate, J., Kale, J. D., and Lal, B. 2006. High resolution daily gridded rainfall data for the Indian region: Analysis of break and active monsoon spells. *Curr. Sci.* 91: 296–306.

Rajeevan, M., Jyoti, B., and Kale, J. D. 2005. *Development of High Resolution Daily Gridded Rainfall Data for the Indian Region*. India Meteorological Department, Report No. 22. New Delhi.

Rajendran, K., Kitoh, A., Srinivasan, J., Mizuta, R., and Krishnan, R. 2012. Monsoon circulation interaction with Western Ghats orography under changing climate. *Theor. Appl. Climatol.* 110 (4): 555-571.

Ramesh, K. V. and Goswami, P. 2007. *The Shrinking Indian summer Monsoon.* Research Report RR CM 0709, CSIR Centre for Mathematical Modelling and Computer Simulation, Bangalore.

Rodwell, M. J. and Hoskins, B. J. 1996. Monsoons and the dynamics of deserts. *Q. J. R. Meteorol. Soc.* 122: 1385–1404.

Ruddiman, W. F. 2003. The anthropogenic greenhouse era began thousands of years ago. *Clim. Change,* 61 (3): 261-293

Santos, E. B., Lucio, P. S., and Santos e Silva, C.M. 2016. Estimating return periods for daily precipitation extreme events over the Brazilian Amazon. *Theor. Appl. Climatol.* 126 (3): 585-595.

Sen, R. S. and Balling, R. C. 2004. Trends in extreme daily precipitation indices in India. *Int. J. Climatol.* 24: 457–466.

Sharda, V. N. and Bhushan, L. S. 1985. Probability analysis of annual maximum daily rainfall for Agra. *Indian J. of Soil Cons.* 13 (1): 16-20.

Shenoi, S. S. C., Shankar, D., and Shetye, S. R. 2002. Differences in heat budgets of the near-surface Arabian Sea and Bay of Bengal: Implications for the summer monsoon. *J. Geophys. Res. Oceans.* 107: 3052-3062.

Shepard, D. 1968. A two-dimensional interpolation function for irregularly spaced data. In: proceedings of the 23rd ACM national conference, January 1968, ACM. pp.517–524.

Singh, N. and Sontakke, N. A. 2002. On climatic fluctuations and environmental changes of the Indo-Gangetic Plains, India. *Clim. Change*, 52 (3): 287–313.

Singh, R. K. 2001. Probability analysis for prediction of annual maximum rainfall of Eastern Himalaya (Sikkim mid hills). *Indian J. Soil Cons.* 29: 263-265.

Stephenson, D. B., Kumar, R.K., Doblas-Reyes, F. J., Royer, J.F., Chauvin, F., and Pezzulli, S. 1999. Extreme daily rainfall events and their impact on

ensemble forecasts of the Indian monsoon. *Mon. Weather Rev.* 127: 1954–1966.

Subash, N. and Sikka, A. K. 2014. Trend analysis of rainfall and temperature and its relationship over India. *Theor. Appl. Climatol.* 117: 449–462.

Subash, N., Sikka, A. K., and Ram-Mohan, H. S. 2011. An investigation into observational characteristics of rainfall and temperature in Central Northeast India—a historical perspective. *Theor. Appl. Climatol.* 103: 305–319.

Subbiah, A. 2002. *Initial Report on the Indian Monsoon Drought of 2002.* Asian Disaster Preparedness Center. 31p.

Sugahara, S., Da-Rocha, R. P. and Silveira, R. 2009. Non-stationary frequency analysis of extreme daily rainfall in Sao Paulo, Brazil. *Int. J. Climatol.* 29: 1339–1349.

Suppiah, R. and Hennessy, K. J. 1998. Trends in total rainfall, heavy rain events and number of dry days in Australia. *Int. J. Climatol.* 18: 1141–1164.

Thomas, T., Gunthe, S. S., Ghosh, N. C., and Sudheer, K. P. 2015. Analysis of monsoon rainfall variability over Narmada basin in central India: Implication of climate change. *J. Water Clim. Change,* 6 (3): 615-627.

Upadhaya, A. and Singh, S. R. 1998. Estimation of consecutive days maximum rainfall by various methods and their comparison. *Indian J. Soil Cons.* 26 (2): 193-201.

Webster, P. J., Magana, V. O., Palmer, T. N., Shukla, J., Tomas, R. A., and Yanai, M. 1998. Monsoons: Processes, predictability, and the prospects for prediction. *J. Geophys. Res.* 103 (C7): 14451–14510.

Yue, S. and Wang, C. 2004. The Mann-Kendall test modified by effective sample size to detect trend in serially correlated hydrological series. *Water Resour. Manag.* 18: 201–218.

TRENDS IN INDIAN SUMMER MONSOON DISTRIBUTION OVER THE WESTERN GHATS

ABHIJIT ASOKAN

(2011-20-109)

ABSTRACT OF THE THESIS

Submitted in partial fulfilment of the requirement for the degree

B.Sc.-M.Sc. (Integrated) Climate Change Adaptation

Faculty of Agriculture

Kerala Agricultural University, Thrissur

ACADEMY OF CLIMATE CHANGE EDUCATION AND RESEARCH

VELLANIKKARA, THRISSUR – 680656

KERALA, INDIA

2016

ABSTRACT

The Western Ghats with its strategic position plays a great role in channelling the summer monsoon rain into the mainland. The natural ecosystems and human livelihoods of this region are highly dependent on the Indian Summer Monsoon rainfall and even the slightest change can trigger a change in these systems. The global climate changing scenario is having its toll in the monsoonal system over this region. The extreme events in the region have been analysed for trends using Mann Kendall method and the return periods of the one day maximum rainfall has been modelled using Generalized Extreme Value (GEV) theory.

The mean annual monsoonal rainfall over the region is 1616.15 mm and the standard deviation is 242.966.It was observed that the mean annual monsoonal rainfall varied from 231.4mm in grid 117 to 3416 mm in grid 253. The one day maximum rainfall extracted from the 32 constituent grids for the entire period showed a variation from 118.63 mm in 1981 to 316.63 mm in 2005. The temporal variation in one day maximum rainfall for the time series had a significant trend. The values were seen to increase steadily and a profound increase was observed in the recent decades. When the One day maximum rainfall was analysed for different latitudes, two latitudes (14°N and 21°N) had significant positive trends in One Day Maximum Rainfall in the whole region. Out of the 32 grids, 7 grids (186, 359, 394, 428, 429, 497 and 498) showed a significant rising trend in one day maximum rainfall. It was also observed that during the recent years, the occurrence of One day maximum Rainfall has shifted to the far end of the season.

The number of grids getting heavy, very heavy and extreme rainfall events was found to have increased during the later years of the study. No significant trend in the instances of occurrence of heavy rainfall over the years was observed. But a significant trend was observed in the occurrences of rainfall events of very heavy and extreme magnitudes. When Split period analysis of the contribution of moderate and high intensity rainfalls was carried out, it was observed that the share of high intensity rainfalls had increased and a decrease was observed in the share of moderate events over the years. The return period analysis of the one day maximum rainfall events was done and it was observed that the 2 year, 5 year, 10

year, 25 year, 50 year and 100 year return levels of rainfall as 186.2mm, 224.3 mm, 250.2 mm, 283.8 mm, 309.3 mm and 335.1 mm for the complete region. The return levels for the two year return period were seen to be over 100 mm for the grids of 184 (118mm), 219 (114.9mm), 253 (145.8mm), 285 (104.5mm), 357 (147.6 mm), 392 (144.2mm), 427 (129.9mm) and 462 (122.4mm).

A significant rising trend in the extreme events of summer monsoon rainfall over the Western Ghats was observed. This calls for better planning in all areas of livelihoods and management strategies to contain the disasters of a changing climate.